CHAPTER 4

Inferred Lifetimes from Observed Trace-Gas Distributions

Lead Authors:
Andreas Engel
Elliot L. Atlas

Co-Authors:
Peter F. Bernath
Harald Bönisch
Alex Brown
Johannes Laube
Kenneth R. Minschwaner
Stephen A. Montzka
Simon O'Doherty
Ronald G. Prinn
Matthew Rigby
Susan M. Schauffler
C. Michael Volk
Shari A. Yvon-Lewis

CHAPTER 4

Inferred Lifetimes from Observed Trace-Gas Distributions

Contents

4.1 Introduction

Atmospheric trends of trace gases are controlled by the balance of sinks (=losses) and sources (including direct emissions). One measure of the rate of loss of any atmospheric constituent is its atmospheric lifetime. A detailed discussion on the distinction between different ways of evaluating lifetimes (e.g., transient and steady-state lifetime) is given in Chapter 2. Species may have multiple different sink processes, and the combination of these processes determines the overall lifetime. For many long-lived species (e.g., chlorofluorocarbons (CFCs)), photochemical breakdown in the stratosphere is the main loss process and, in this case, the stratospheric lifetime becomes the overall atmospheric lifetime. In the troposphere, oxidation – often initiated by the hydroxyl radical (OH) – as well as wet and dry deposition processes are major loss processes. Some chemicals become destroyed in the hydrosphere or in soils, and these losses also must be considered to properly estimate their lifetimes. This chapter discusses the derivation of atmospheric lifetimes using atmospheric measurements of trace gases and model studies which are closely linked to atmospheric observations. Observations of global trace-gas mole fractions and their temporal change, of trace gas atmospheric distributions, and of the atmospheric mole fraction correlations in regions where destruction dominates atmospheric variability (e.g., in the stratosphere) can all be used to derive measurement-based lifetimes. They can also serve to constrain model estimates of atmospheric lifetimes and environmental impacts.

The atmospheric distribution of a trace gas, its temporal trends and its variability depend in part on the atmospheric lifetime. In the simplest case of a species whose emission into the atmosphere has stopped and which has no other sources, insight into a chemical's lifetime is provided by the e-folding time of the decrease of the atmospheric mole fraction. The most notable example of this is methyl chloroform, whose global mean mole fraction has decreased at an approximately constant exponential rate since 1998 (Montzka *et al.,* 2011). The e-fold time derived from exponential decay, however, is not generally the same as that derived for steady-state conditions, which is what models typically derive for trace gases. Lifetimes derived from observations are often affected by such temporal changes and are usually not steady-state lifetimes. Usually, even for species of anthropogenic origin that are no longer emitted in large amounts into the atmosphere, there will be some sources so that the simple e-folding time will seldom be a direct measure of the lifetime. In such cases a combination of different modeling techniques with observations of atmospheric mole fractions (see Section 4.3) can be used to derive optimal estimates of lifetimes of a trace gas. Note, however, that the lifetime derived in this way is usually not a steady-state lifetime but rather an average of the transient lifetimes over the time period considered for the respective study. In many cases the differences will be rather small, as discussed in the individual section of this chapter and in Chapter 2 and these calculated transient lifetimes can be transformed to yield steady-state lifetime estimates.

In this chapter we will present results from techniques that interpret atmospheric measurements of trace gases in different ways. Common to all methods is the need for well-calibrated, high-quality data. In Section 4.2 we thus present available tropospheric and stratospheric observations. The tropospheric measurements used in this report primarily rely on results from two global atmospheric monitoring networks (National Oceanic and Atmospheric Administration/Earth System Research Laboratory (NOAA/ESRL) and Advanced Global Atmospheric Gases Experiment (AGAGE)), though other network data are available for some of the gases evaluated here (e.g., the University of California at Irvine (UC Irvine) (http://cdiac.ornl.gov/trends/otheratg/blake/blake.html, the University of East

Anglia (UEA), and the SOGE (System for Observation of halogenated Greenhouse gases in Europe) networks). The section on stratospheric observations is subdivided into *in situ* data from high-altitude aircraft and from balloons (which are usually of high precision and accuracy but have a limited coverage) and satellite data (with less accuracy and higher absolute uncertainties but a much better spatial and temporal coverage). Section 4.3 then discusses the methods that rely on different combinations of observations with modeling work. In Section 4.4 we discuss the applicability of using tracer-tracer correlations observed in the stratosphere to infer relative and absolute stratospheric lifetimes, and we present results from this analysis of correlations. For the calculation of absolute lifetimes from the relative lifetimes of two tracers, the lifetime of one of the two tracers must be specified and the absolute lifetime of the other is reported relative to this specified lifetime. There is also an approach deriving absolute lifetimes from correlation analysis by using mean age as one of the tracers in the correlation (Volk *et al.,* 1997). The applicability of this method is discussed in more detail in Chapter 2 and will not be pursued any further in the present chapter.

4.2 Database of Atmospheric Observations

4.2.1 Tropospheric Observations

As discussed above, long-term observational records with consistent calibration are needed for the calculation of atmospheric lifetimes (Sections 4.3 and 4.4), to correct observed stratospheric tracer-tracer correlations for tropospheric trends, and to calculate global burdens. Where data from multiple sources are combined, care must be taken that these are intercalibrated well and are consistent with each other over time. Data from two atmospheric monitoring networks are often used for this purpose: the NOAA/ESRL (http://www.esrl.noaa.gov/) and AGAGE (http://agage.eas.gatech.edu/). Table 4.1 lists available data from these networks and others. Annual mean global mole fractions derived from these independent networks are typically within a few percent of each other for the more abundant chemicals (Montzka and Reimann, 2011).

Global tropospheric burdens of long-lived halocarbons and their changes over time are derived from atmospheric measurements of discrete air samples at multiple sites in each hemisphere at Earth's surface. The analysis of light passing through the atmosphere has also allowed trace-gas densities and their changes over time to be derived from satellites and from ground-based instrumentation (see Section 4.2.2). With either approach, measurements are conducted at remote sites to provide observational data for anthropogenically emitted gases that are representative of large atmospheric regions. Discrete measurements are conducted by collecting flasks and sending them to a central laboratory for analysis or by instruments located at remote sites that continually analyze samples as they are collected. Ground-based air sampling networks are designed to capture the predominant mole fraction gradients at Earth's surface so that an accurate estimate of global mean surface mole fractions can be derived. Because not all observation sites are shared by the main sampling networks, bringing data together from different networks can add substantially to our understanding of the surface distribution of a trace gas and provide a more accurate estimate of its true global mean mole fraction. Combining data from different networks is only useful if data from these networks are of comparable quality and if mole fraction differences between networks arising from standardization can be removed. In addition, for inverse techniques to provide accurate information about the distribution of sources (and potentially sinks), differences must be removed if the data are to be combined, so that distributions and time variations in the combined data record reflect true atmospheric gradients and variations.

Table 4.1. Summary of data availability from tropospheric monitoring networks (NOAA=NOAA/ESRL, USA; AGAGE=ALE/GAGE/AGAGE; UEA=University of East Anglia, UK; UCI=University of California, Irvine, USA in the table below). In the NOAA, AGAGE and UCI networks measurements are made at multiple sites in each hemisphere unless otherwise indicated. Dates indicate the year that the measurement started. Compounds are grouped into classes with removal primarily in the stratosphere or in the troposphere. CG=Cape Grim, Tasmania; TH=Trinidad Head/Cape Meares, California; JF=Jungfraujoch, Switzerland; MH=Mace Head/Adrigole, Ireland; CM=Cape Matatula, American Samoa; RP=Ragged Point, Barbados. (U) indicates uncalibrated.

Compound	**Formula**	**NOAA**	**AGAGE**	**Notes**
STRATOSPHERIC REMOVAL Species				
CFC-11	CCl_3F	1978[a]	1978	
CFC-12	CCl_2F_2	1978 [a]	1978	
CFC-113	CCl_2FCClF_2	1992 [b]	1982	CG in 1982, TH in 1984, CM and RP in 1985; and MH in 1987
CFC-114	$CClF_2CClF_2$	N.A.	2003	Includes a {constant} correction for co-elution of CFC-114a
CFC-115	CF_3CClF_2	2007 [c]	1998	AGAGE initially at MH and CG; more sites added in 2005
Carbon tetrachloride	CCl_4	1990 [a]	1978	CG, CM, RP in 1978, TH and MH in 1979
Nitrous oxide	**N_2O**	1978 [a]	1978	
Halon-1211[d,e]	$CBrClF_2$	1992	1994	AGAGE at MH in 1994, CG in 1998 and JF in 2000; more sites added in 2005
Halon-1301[d,e]	$CBrF_3$	1989	1997	AGAGE initially at MH CG in 1998; JF in 2000; more sites added in 2005
Halon-2402[d,e]	$CBrF_2CBrF_2$	1995	2005	NOAA data before 2004 have substantial time gaps
TROPOSPHERIC REMOVAL Species				
Methane[f]	CH_4	1985	1985	TH in 1985, CG in 1986, MH and CM in 1987
Methyl chloroform	CH_3CCl_3	1990	1978	
Methyl chloride	CH_3Cl	1995	1998	AGAGE initially at MH and CG; more sites added in 2005
Methyl bromide	CH_3Br	1995	1998	AGAGE initially at MH and CG; more sites added in 2005
HCFC-22	$CHClF_2$	1992	1998	AGAGE initially at CG; MH in 1999; more sites added in 2005
HCFC-141b	CH_3CCl_2F	1992	199	AGAGE initially at MH; CG in 1998; more sites added in 2005
HCFC-142b	CH_3CClF_2	1992	1994	AGAGE initially at MH; CG in 1998; more sites added in 2005
Halon-1202[d,e]	CBr_2F_2	N.A.	N.A.	
HFC-23[e]	CHF_3	N.A.	2007	
HFC-32	CH_2F_2	2007 [c]	2005	
HFC-125	CHF_2CF_3	2007 [c]	1998	AGAGE initially at MH and CG; more sites added in 2005
HFC-134a	CH_2FCF_3	1994	1994	AGAGE at MH in 1994, CG in 1998; JF in 2000, more sites added in 2005
HFC-143a	CF_3CH_3	2007 [c]	2003	

HFC-152a	CH_3CHF_2	2000 [c]	1994	AGAGE at MH in 1994 and CG in 1998; more sites added in 2005
HFC-227ea	CF_3CHFCF_3	2007 [c]	2006	AGAGE initially at MH and CG; more sites added in 2007
HFC-245fa	$CHF_2CH_2CF_3$	N.A.	2006	AGAGE initially at MH and CG; more sites added in 2007
ADDITIONAL Species				
HFC-365mfc	$CF_3CH_2CF_2CH_3$	2007 [c]	2003	AGAGE initially at MH and JF; CG in 2004; more sites added in 2008
HFC-236fa	$CF_3CH_2CF_3$	N.A.	2006	AGAGE initially at MH and CG; more sites added in 2008
HFC-43-10mee	$CF_3CHFCHFCF_2CF_3$	N.A.	2010 [c] (U)	
CFC-13	$CClF_3$	2007 [c]	2003 [c] (U)	

Additional notes: **N.A.** indicates no measurements being made. NOAA data are derived with flask sampling and *in situ* instrumentation, depending on compound. NOAA results indicated in the table are derived from only flask measurements with the following exceptions: [a] Global means from NOAA are derived from a combination of flask and *in situ* measurements; the *in situ* measurements began in the late 1980s. [b] Global means from NOAA are derived from a combination of flask and *in situ* measurements; the *in situ* measurements began in 1999-2000. [c] Indicates that these data are currently unpublished. [d] Halons-1211 and -2402 are removed both in the troposphere and stratosphere. For Halon-1301 the stratosphere is the main loss region, while Halon-1202 is mainly removed in the troposphere. [e] UEA has CG data available for all four Halons and HFC-23 dating back to 1978 (partly from archived air samples). [f] Earlier CH_4 measurements are available from UCI dating back to 1978.

Although Table 4.1 provides information about on-going measurement records, i.e., chemicals for which measurements are being conducted on a regular basis to observe changes in atmospheric composition as they occur, other archives of air exist that allow an understanding of atmospheric changes in years before measurements began at these sites. One such air archive, the Cape Grim Air Archive, includes canister samples that were collected since 1978. Analysis of this air archive with present-day analysis techniques has provided an understanding of atmospheric composition changes in years since 1978 (e.g., Oram *et al.,* 1995; Maiss *et al.,* 1996; Prinn *et al.,* 2000). Other natural air archives also exist that have extended the measurement record into the early 1970s (e.g., Mühle *et al.,* 2010). Air trapped in consolidated snow (firn) or in ice bubbles has been extracted and atmospheric mole fractions of halocarbons have been measured as a function of depth (age) in snow and ice. The mean age of air samples collected from firn are up to ~100 years old (Severinghaus *et al.,* 2010). Although deriving an atmospheric history is less straightforward from firn or ice-bubble air than from air archived in canisters, past atmospheric changes can be reliably derived (e.g., Martinerie *et al.,* 2009; Buizert *et al.,* 2012).

4.2.2 Stratospheric Observations

Stratospheric observations of halocarbon mole fractions are important in several respects when determining lifetimes:

(i) the observed correlation slope between mole fractions of two species at or near the tropopause can be used to derive the relative lifetimes of two species (see Section 4.4),

(ii) the vertical distributions, which are a function of lifetime and growth rate, can be used to constrain model calculations which are used to derive lifetimes (see Chapter 5),

(iii) from global distributions of a tracer and modeled loss rates, the lifetime can be inferred (Section 4.3.4), and

(iv) stratospheric observations are needed to determine the stratospheric contribution to the total atmospheric burden of a species, which is needed to calculate the lifetime.

For determination of the slope of the correlation between two gases (point (i) above), high accuracies and sufficient data coverage are needed near the tropopause (see Chapter 2 and Section 4.4). Clearly, the slope correlation method requires simultaneous observations of at least two compounds. Moreover, observations with sufficient precision have only become available since the 1990s onward for most of the compounds considered here. Measurements can be made either *in situ* using high-flying aircraft or balloons as platforms or by remote sensing from space. Note that for the purpose of this section on stratospheric data the term *in situ* will include data from flask sampling techniques as well as from direct *in situ* measurements, as the characteristics of the data are similar.

4.2.2.1 *In Situ* Stratospheric Data

Due to the complexity involved with bringing instruments into the stratosphere, stratospheric *in situ* data are sporadic in time and do not have global coverage in space. Their main advantage is that they are often characterized by high spatial resolution and high data quality with systematic uncertainties that are usually rather small. In contrast to tropospheric observations which are available for many species on a regular basis, stratospheric *in situ* observations of a number of gases are available on campaign basis, i.e., only sporadic in time and space.

A number of publications focus on the stratospheric measurements of methane (CH_4) and nitrous oxide (N_2O) (Herman *et al.,* 1998, 2003; Park *et al.,* 2004; Spackman *et al.,* 2007) resulting in a broad database from a variety of campaigns, platforms and instruments. The most extensive data compilations for these two compounds are given by Andrews *et al.* (2001) and Greenblatt *et al.* (2002) who combine aircraft, balloon and (for the latter) satellite observations.

There are also publications reporting CFC-11 (CCl_3F) and/or CFC-12 (CCl_2F_2) mole fractions in the stratosphere. Examples are Ray *et al.,* 1999, 2002; Bujok *et al.,* 2001; Richard *et al.,* 2001; Jost *et al.,* 2002; Plumb *et al.,* 2003; Ehhalt *et al.,* 2007; Homan *et al.,* 2010, and Werner *et al.,* 2010. The other major ozone depleting compounds – carbon tetrachloride (CCl_4), methyl chloroform (CH_3CCl_3), and HCFC-22 ($CHClF_2$) – have been examined in Jobson *et al.,* 1999; Sen *et al.,* 1999; Toon *et al.,* 1999; and Park *et al.,* 2010. The most suitable data for stratospheric lifetime estimation for the latter five compounds in terms of data density and quality have been presented in Volk *et al.,* 1996, 1997; Moore *et al.,* 2003 (both excluding HCFC-22); Schauffler *et al.,* 2003; and Laube *et al.* (2013).

There are considerably less stratospheric data available for other compounds except for Halon-1211 ($CBrClF_2$) and CFC-113 (CCl_2FCClF_2), which have been measured frequently in the stratosphere since the 1990s (e.g., Volk *et al*., 1996, 1997; Wamsley *et al.,* 1998; Flocke *et al.,* 1999; and Moore *et al.,* 2003). There are only six papers reporting good quality data for Halon-1301 ($CBrF_3$) and/or CFC-115 ($CClF_2CF_3$) (Wamsley *et al.,* 1998; Schauffler *et al.,* 1999, 2003; Pfeilsticker *et al.,* 2000; Laube *et al.,* 2008, 2010a.)

Stratospheric observations of many of the remaining compounds are reported by Wamsley *et al.,* 1998 (methyl bromide (CH_3Br), Halon-2402 ($CBrF_2CBrF_2$)), Flocke *et al.,* 1999 (CFC-114 ($CClF_2CClF_2$) and Halon-2402), Schauffler *et al.,* 1999 (CH_3Br, Halon-2402), Schauffler *et al.,* 2003 (CFC-114, CFC-114a (CCl_2FCF_3), HCFC-141b (CH_3CCl_2F), HCFC-142b (CH_3CClF_2)) Ehhalt *et al.,* 2007 (CH_3Cl), Laube *et al.,* 2008, 2010a (CFC-114, CFC-114a, HCFC-141b, HCFC-142b, Halon-2402, Halon-1202 (CBr_2F_2)), Park *et al.,* 2010 (HCC-40 (CH_3Cl) and CH_3Br), Pfeilsticker *et al.,* 2000, and Sturges *et al.,* 2000 (Halon-2402, Halon-1202, CH_3Br). In addition, for other HFCs the only published observations are those of HFC-227ea (CF_3CHFCF_3) in Laube *et al.,* 2010b. No stratospheric data has yet been reported for a number of the compounds that were selected for evaluation in this report. One report for HFC-23 (CHF_3) is Oram *et al.,* 1998. The compounds for which there is no reported stratospheric data include HFC-32 (CH_2F_2), HFC-125 (CHF_2CF_3), HFC-134a (CH_2FCF_3), HFC-143a (CH_3CF_3), HFC-152a (CH_3CHF_2), and HFC-245fa ($CHF_2CH_2CF_3$).

4.2.2.2 Satellite Observations

Measurements of trace gases from satellites are obtained with techniques that employ two basic viewing geometries: nadir and limb-viewing sounders. Nadir sounders view the Earth's surface directly beneath the satellite sensor, while limb sounders look through an oblique slice of the atmosphere without viewing the surface. Nadir sounders such as IRIS, IMG, AIRS, TES and IASI are capable of measuring the total column of CFC-11, CFC-12, HCFC-22 and CH_4. Unfortunately these instruments do not have sufficient vertical resolution to be used for lifetime calculations. In contrast, limb sounders have sufficiently high vertical resolution to allow the calculation of the stratospheric lifetime of long-lived species from tracer-tracer correlations or from photolysis rate calculations. The instruments of primary interest for this study are ATMOS, CIRRIS-1A, CRISTA-2, CLAES, MIPAS, ACE, HIRDLS and MLS.

Atmospheric Trace Molecule Spectroscopy Experiment (ATMOS): ATMOS was designed to measure the volume-mixing ratio (VMR) of atmospheric constituents active in the infrared spectral region (IR). The ATMOS instrument was a Fourier transform spectrometer carried onboard NASA space shuttles on four occasions (1985, 1991, 1992 and 1993). ATMOS was capable of measuring vertical profiles of CFC-11, CFC-12, CCl_4, HCFC-22, CH_3Cl, N_2O and CH_4. Measurements of CH_3Cl, CFC-12, CFC-11, HCFC-22 and CCl_4 from ATMOS were first reported in Zander *et al.* (1987).

Measurements of N_2O, CFC-11, CFC-12 and CCl_4 VMRs from ATMOS were compared to those made by the NASA ER-2 aircraft during November 1994 (Chang *et al.,* 1996). The mean difference in CFC-11 VMRs between ATMOS and ER-2 was +4%, which is well within the uncertainty of the satellite measurements. Agreement for CFC-12 ranged between + 5% and – 6%, just a little outside the estimated ATMOS measurement precision of 5%. ATMOS measurements of CCl_4 were systematically higher (15%) than *in situ* measurements. In 2002 ATMOS version 3 data was released (Irion *et al.*, 2002). Retrievals in version 3 extended further into the troposphere than those in version 2, which has allowed better comparison with tropospheric *in situ* measurements. These comparisons showed good agreement for CFC-11, CFC-12, HCFC-22 and CH_3Cl although comparisons for CCl_4 showed that ATMOS VMRs remained high.

Cryogenic Infrared Radiance Instrumentation for Shuttle (CIRRIS): CIRRIS was designed to measure the atmospheric IR radiance from the troposphere to the lower thermosphere. The instrument was flown onboard the shuttle between April 28th and May 6th 1991. VMR profiles were retrieved for CFC-11 between 13 and 25 km and between 13 and 34 km for CFC-12 (Bingham *et al.,* 1997). Retrievals of atmospheric CCl_4 were also carried out using CIRRIS data between 10 and 20 km.

Cryogenic Infrared Spectrometers and Telescopes for the Atmosphere (CRISTA): CRISTA flew two missions onboard the Astronomical Shuttle Pallet Satellite (ASTRO-SPAS) in November 1994 (CRISTA-1) and in August 1997 (CRISTA-2). CRISTA analyzed IR emission from the Earth's limb for about 8 days during each flight. Vertical profiles from the upper troposphere to the lower thermosphere were retrieved from these measurements. CRISTA-2 was capable of measuring vertical profiles of CH_4, N_2O, CFC-11 and CFC-12 (Grossmann *et al.,* 2002). CFC-11 was retrieved between 8 and 28 km (Kuell *et al.,* 2005) and the VMRs agreed within the estimated errors with measurements made by the BONBON whole air sampler. Global CFC-11 VMR fields were produced on a 2 km x 5° latitude grid.

Cryogenic Limb Array Etalon Spectrometer (CLAES): CLAES on NASA UARS obtained global distributions of CFC-12 and CFC-11 in the stratosphere between October 1991 and May 1993. Seasonally varying dynamical features similar to those from N_2O and CH_4 were observed. These global distributions were compared and showed good agreement with the Goddard Space Flight Centre (GSFC) two-dimensional (2-D) model (Roche *et al.,* 1998). Instantaneous lifetimes were calculated for CFC-12 and N_2O using the global loss rates from four separate seasons and the mean atmospheric burden during this time. The calculated instantaneous lifetimes were 114 ± 22 years (CFC-12) and 118 ± 25 years (N_2O). These values led to steady-state lifetimes of 103 ± 25 years (CFC-12) and 117 ± 26 years (N_2O) (Minschwaner *et al.,* 1998). Section 4.3.4 of this chapter presents new results for the CFC-11 lifetime using this method applied to more recent satellite measurements.

Michelson Interferometer for Passive Atmospheric Sounding (MIPAS): MIPAS onboard ENVISAT was, until April 2012, capable of measuring the atmospheric concentration of CFC-11, CFC-12, HCFC-22, N_2O and CH_4. Retrievals carried out by Moore *et al.* (2006) calculated vertical profiles up to 24 km for CFC-11 and 27 km for CFC-12. HCFC-22 was also retrieved from MIPAS data producing a vertical profile up to a maximum altitude of 18 km. Hoffmann *et al.* (2005) also retrieved CFC-11 and CFC-12 from MIPAS with total errors of 7 to 10% in the upper troposphere and lower stratosphere. Hoffmann *et al.* (2008) carried out additional work on CFC-11 and satisfactory comparisons were made with retrievals from ATMOS, CRISTA and CIRRIS. Comparisons with the *in situ* High Altitude Gas Analyser (HAGAR) showed differences of less than 10% between HAGAR and MIPAS CFC-11.

Atmospheric Chemistry Experiment (ACE): ACE Fourier transform spectrometer (FTS) was launched onboard the satellite SCISAT-1 in August 2003(Bernath, 2006). ACE-FTS is capable of retrieving concentrations of CCl_4, CFC-11, CFC-12, CFC-113, CH_3Cl, HCFC-22, HCFC-141b, HCFC-142b, N_2O and CH_4. Carbon tetrachloride (CCl_4) was first retrieved from ACE observations for the 2004 global stratospheric chlorine budget derived by Nassar *et al.* (2006a) and a global distribution was determined by Allen *et al.* (2009). Brown *et al.* (2011) derived trends for 16 halogenated gases.

Validation of ACE-FTS version 2.2 (V.2.2) measurements of CFC-11 were made by comparison with balloon-borne FTS measurements (Mahieu *et al.,* 2008). Comparisons with the FIRS-2 instrument showed agreement to within 10% below 16 km. ACE-FTS measurements were also compared to the Mk-IV instrument, with agreement to 10% above 12 km and 20% below 12 km. CFC-11 was used in both the global stratospheric fluorine and chlorine budgets (Nassar *et al.* 2006a, 2006b). Validation of ACE-FTS V.2.2 measurements of CFC-12 also were made by comparisons with balloon-borne FTS measurements (Mahieu *et al.,* 2008) and the agreement is similar to the CFC-11 case. The retrieval method for CFC-113 was outlined by Dufour *et al.* (2005). This was the first retrieval of CFC-113 from a space-based instrument and was within 15% of surface mole fractions measured by AGAGE.

HCFC-141b is a new species available from the version 3.0 ACE-FTS retrieval. The retrieval method used by ACE for HCFC-142b was described by Dufour *et al.* (2005), who found that there was agreement to 15% between ground-based AGAGE and ACE measurements.

Other Satellites: Whilst active the High Resolution Dynamics Limb Sounder (HIRDLS) instrument retrieved both CFC-11 and CFC-12 (http://www.eos.ucar.edu/hirdls/data/). The Microwave Limb Sounder (MLS) retrieves both N_2O and CH_3Cl.

4.3 Combined Model/Observational Approaches

This section discusses different applications that use modeling in combination with observations and other relevant data to derive atmospheric lifetimes. The first application is inverse modeling to estimate lifetimes. Inverse modeling uses observational data measured at long-term monitoring sites (and potentially other relevant measurements) in combination with a transport model to infer emissions and/or lifetimes. For the study here, emissions are specified and a 2-D model is applied. This technique is used for the longer-lived species (lifetime more than 5 years) with predominately anthropogenic sources.

Forward modeling or global box modeling approaches can be applied to shorter-lived compounds with natural sinks and sources. For longer-lived compounds forward modeling can generally be used to check if lifetimes and assumed emissions are in agreement with the observed tropospheric time series. Global box modeling studies are discussed with respect to CH_3Cl, CH_3Br and CCl_4 in this report.

The inverse and forward modeling approaches require the use of independent bottom-up emission data. Industry reported production numbers are available up to the year 2007 from the Alternative Fluorocarbons Environmental Acceptability Study (AFEAS) for CFCs, HCFC-22, -124, -141b, and -142b, as well as for HFC-134a, -125, and -143a. However, AFEAS stopped their work as less than half of the global sales are now from companies reporting to AFEAS, so total emissions are not captured. Emissions used for this report are discussed in Section 4.3.1, and are consistent with modeling runs discussed in Chapter 5 of this report. No updated emission data were developed for this assessment.

The last approach used in this section will use global scale measurements of trace-gas distributions to estimate global atmospheric burdens. Global loss rates of the trace gas are then estimated from model calculations using recommended loss rates. The ratio of global burden to global loss rate is a direct measure of the instantaneous atmospheric lifetime at the time of the measurement.

4.3.1 Inverse Modeling

When combined with emissions estimates and knowledge of large-scale atmospheric chemistry and transport processes, trends in background mole fractions can be used to determine the overall lifetime of atmospheric constituents. Previous "inverse" estimates of the transient lifetimes of CFC-11, CFC-12, and CH_3CCl_3 have been made using AGAGE and NOAA measurements, emissions inventories and a simplified model of atmospheric transport and chemistry (Cunnold *et al.,* 1983, 1994; Prinn *et al.,* 2001, 2005).

Rigby *et al.* (2013) follow an approach similar to Cunnold *et al.* (1983), in which a two-dimensional chemical transport model (CTM) was used to simulate atmospheric mole fractions, which were compared to AGAGE and NOAA observations between 1978 and 2011. Using a Bayesian inverse method they combined the measurements and model to improve prior estimates of a set of parameters related to overall trace-gas lifetimes (stratospheric loss frequencies, OH concentrations, initial mole fractions and model transport parameters) in order to better match the observations. Lifetimes were estimated only for CFC-11, -12, -113, and CH_3CCl_3 as relatively robust emissions estimates were thought to exist for these compounds (McCulloch *et al.,* 2001; 2003, Rigby *et al.*, 2013). The lifetimes of other gases, with more poorly understood emissions (e.g., CCl_4, Xiao *et al.,* 2010a, Montzka and Reimann*,* 2011) were not estimated with this method.

4.3.1.1 Two-Dimensional Modeling of CFC and CH_3CCl_3 Mole Fractions

To simulate mole fractions at AGAGE and NOAA sampling sites, Rigby *et al.* (2013) used a 2-dimensional model of atmospheric transport and chemistry based on that of Cunnold *et al.* (1983, 1994). The model parameterizes the transport of trace gases between "boxes" with latitudinal boundaries at 30°N, 0°N and 30°S and vertical boundaries at 200hPa and 500hPa. Initial estimates for the model transport parameters were taken from Cunnold *et al.* (1983, 1994) and the eddy diffusion parameters were subsequently adjusted in the inversion. Reaction rates of the gases with the tropospheric hydroxyl radical were taken from Chapter 3 recommendations. Stratospheric destruction was parameterized by loss frequencies in each of the four stratospheric boxes.

Emissions into the model were based on the methodology of McCulloch *et al.* (2001, 2003), who used surveys such as AFEAS, along with estimates of the consumption in all countries reported to the United Nations Environment Programme (UNEP) and assumptions about releases from banks to estimate global emissions. The estimates were compiled in 2006, and include projections to 2100, based on agreed phase-out schedules. These emissions were not adjusted in the Rigby *et al.* (2013) inversions. However, estimates of the influence of errors in the emissions on lifetimes were included in the derived uncertainty estimates.

4.3.1.2 Inverse Method

Rigby *et al.* (2013) used an inverse approach to estimate stratospheric loss frequencies for CFC-11, -12, and -113 at the same time as model transport parameters, OH concentrations and initial conditions. A non-linear (quasi-Newton) Bayesian inversion framework was used in which prior estimates of this set of parameters were provided, with estimates of their uncertainty. These parameters were subsequently adjusted in the inversion to bring the model prediction of the atmospheric mole fractions into better agreement with the observations, taking into account measurement and model uncertainties.

Initial estimates of the stratospheric loss frequencies of CFC-11, -12, and -113 were adjusted so that stratospheric lifetimes matched current World Meteorological Organization (WMO) recommendations (45, 100, and 85 years, respectively). The uncertainty in these stratospheric lifetimes was estimated from the range in overall lifetimes from previous photochemical model inter-comparison studies (Park *et al.,* 1999). The *a priori* global lifetime of CH_3CCl_3 was determined by the *a priori* global OH concentration (Spivakovsky *et al.*, 2000), assumptions about oceanic uptake (Butler *et al.*, 1991), and the assumed CH_3CCl_3 stratospheric loss frequencies (Naik *et al.*, 2000).

4.3.1.3 Lifetime Estimates and Optimized Mole Fractions

Two sets of inversions were performed, one using AGAGE data and another using NOAA data. Optimized mole fractions for the AGAGE inversion at the four surface boxes are shown in Figure 4.1. Optimized steady-state lifetimes are given in Table 4.2. Rigby *et al.* (2013) note that the influence of errors in estimated emissions is very large during the 1980s and 1990s, when emissions were high. Therefore, to minimize the influence of un-accounted emissions, the lifetimes presented below are the average taken from the time of peak burden onwards for each gas, until the end of 2011.

Rigby *et al.* (2013) estimate a steady-state lifetime for CFC-11 of 54 (42-73) years when AGAGE data were used and 52 (38-70) years when NOAA data were used (2-σ uncertainties). These estimates are somewhat longer than, but not significantly different from, the 45-year lifetime recommended in recent WMO reports (Prinn *et al.,* 1999). The uncertainties in these estimates include the influence of errors in the observations and *a priori* parameters, as well as an estimate of the influence of potentially biased emissions and calibration scales on the derived lifetimes (Rigby *et al.*, 2013).

Similarly to CFC-11, the Rigby *et al.* (2013) estimates of the lifetime of CFC-113 (109 (89-133) and 109 (86-140) years for AGAGE and NOAA, respectively) are longer than the values given in WMO Ozone Assessment Reports going back to the 1990s (85 years). However, they are in agreement with Volk *et al.* (1997), who estimated a lifetime of 112 ± 31 years (based on a lifetime for CFC-11 of 50 years) using observations of CFCs in the stratosphere. The steady-state lifetime of CFC-12 (111 (80-154) and 112 (78-160) years for AGAGE and NOAA, respectively) and CH_3CCl_3 (5.04 (4.78-5.33) years and 5.04 (4.71-5.42)) are consistent with recommended values in recent WMO assessments and other recently published estimates (e.g., Volk *et al.*, 1997, Prinn *et al.*, 2005).

The inversion method was also evaluated against output from the Whole Atmosphere Community Climate Model (WACCM) model (See Chapter 5). In this flux-based model calculation, mole fractions of several halocarbons at the AGAGE stations were used as the input to the inversion model together with the emissions used in the model. The resulting lifetimes calculated for CFC-11 were in very good agreement to the WACCM calculated lifetime, and lifetimes derived for CFC-12 and CH_3CCl_3 with the inversion were in good agreement (differences below 10%) with the model-derived values.

Table 4.2. *A priori* and optimized lifetimes (years) deduced using AGAGE and NOAA measurements. Figures in brackets indicate the 2-σ uncertainty ranges**.**

Species	**Lifetime (years)**		
	A priori	**AGAGE**	**NOAA**
CFC-11	45 (29-75) [1]	54 (42-73)	52 (38-70)
CFC-12	100 (71-170) [1]	111 (80-154)	112 (78-160)
CFC-113	85 (58-140) [1]	109 (89-133)	109 (86-140)
CH_3CCl_3	5.0 (2.8-10.5) [2]	5.04 (4.78-5.33)	5.04 (4.71-5.42)
CH_3CCl_3 with respect to OH loss	6.14 (4.0-11.6)	6.13 (5.24-7.39)	6.12 (5.23-7.37)

[1] Target global lifetime (WMO 2010 recommendation (Montzka and Reimann., 2011)) obtained by tuning initial stratospheric lifetime in the 12-box model. Uncertainty ranges are estimated based on Park *et al.*, 1999.

[2] 12-box model-calculated lifetimes based on OH concentrations from Spivakovsky *et al.* (2000), OH reaction rates recommended in Chapter 3 and stratospheric lifetimes from Naik *et al.,* 2000. Uncertainty range based on 100% uncertainty in OH concentration in each model semi-hemisphere.

4.3.1.4 Lifetimes of Gases Primarily Destroyed by Tropospheric OH

Using the tropospheric OH fields and transport parameters derived above, the 12-box model was used to simulate atmospheric concentrations of long-lived radiatively important trace gases that are primarily destroyed by tropospheric OH: CH_4, and the major HCFCs and HFCs. Simulations were performed from the time of peak CH_3CCl_3 burden to the end of 2011, and the mean steady-state lifetime of each gas during this period was estimated. Reaction rates with OH were taken from Chapter 3, and stratospheric lifetimes were taken from the 2-D model simulations in Chapter 3. Uncertainties in the derived lifetimes were due to the uncertainties in the tropospheric OH field, reaction rates and stratospheric lifetimes. The uncertainty in the derived OH field includes the measurement and modeling uncertainty propagated through the inversion and the uncertainty due to the prescribed CH_3CCl_3 stratospheric loss and oceanic uptake lifetimes and the CH_3CCl_3-OH reaction rate. This leads to an overall error in our OH estimates of approximately 13.8% (1 σ). The influence of uncertainties in OH, reaction rates, and stratospheric loss rates on the lifetimes of the related species was made by independently perturbing each term in the model, and tracking the resulting change in steady-state lifetime. Table 4.3 summarizes these calculations.

4.3.2 Other Models – Halons

While, in general, model-derived values of atmospheric lifetimes will be discussed in Chapter 5 of this report, there is one study which discusses the stratospheric lifetimes of Halons and in particular gives some insight into the stratospheric lifetimes of Halon-2402 and Halon-1202 (Newland *et al.*, 2012) which is closely linked to atmospheric observations. In this study a 2-D model approach using measured trends from the Cape Grim archive has also been applied to estimate the emissions and lifetimes of the four Halon species: Halon-1211, Halon-1301, Halon-2402, and Halon-1202 (Newland *et al.,* 2012). For the tropospheric lifetimes, the model was run to steady state with OH loss and photolysis active only in the troposphere, and the global burden of each trace gas was divided by the estimated global emission. Stratospheric lifetimes in Newland *et al.* (2012) were taken from Laube *et al.* (2013) for Halon-1211 and Halon-1301, and model parameters evaluated against available balloonborne measurements of Halons in the stratosphere for Halons-2402 and -1202. The partial steady-state lifetimes for stratospheric loss derived in this way are 31 (27-37) years and 21 (18-26) years for Halons-2402 and -1202, respectively (see also Table 4.10).

Table 4.3. Lifetimes of CH_4 and the major HCFCs and HFCs based on the OH concentration derived in the 12-box model inversion, modeled stratospheric lifetimes and reaction rates from Chapter 3. The table shows both the global lifetime and lifetime with respect to tropospheric OH loss. 2-σ uncertainties are shown in parentheses.

Gas	Tropospheric OH lifetime (years)	Global lifetime (years)
CH_4	10.5 (8-15.1)	9.8 (7.6-13.8)
HCFC-22	13.2 (9.9-20.1)	12.4 (9.3-18.5)
HCFC-141b	10.7 (8-16.1)	9.4 (7.2-13.6)
HCFC-142b	19.4 (13.8-33.1)	17.7 (12.7-29.2)
HFC-23	244 (169-438)	228 (160-393)
HFC-32	5.65 (4.2-8.61)	5.4 (4-8.1)
HFC-125	32.5 (23.6-52.3)	30.5 (22.2-48.9)
HFC-134a	14.3 (10.4-23)	13.5 (9.9-21.2)
HFC-143a	57.2 (41.3-92.9)	51.4 (37.7-80.4)
HFC-152a	1.65 (1.26-2.39)	1.6 (1.2-2.2)
HFC-227ea	38.3 (26.7-67.6)	35.8 (25.4-60.7)
HFC-245fa	8.41 (5.8-15.31)	7.9 (5.5-13.8)

4.3.3 Global Box Models

Simple global box modeling has been used to examine the lifetimes of methyl bromide (Hu *et al.,* 2012; Yvon-Lewis and Butler, 2002; Yokouchi *et al.,* 2000; Yvon-Lewis and Butler, 1997; Yvon and Butler, 1996; Butler, 1994), methyl chloride (Hu *et al.,* 2013; Xiao *et al.,* 2010b; Yvon-Lewis and Butler, 2002) and carbon tetrachloride (Yvon-Lewis and Butler, 2002) (Table 4.4).

The global pseudo first order loss rate constants (k_{ocn}, k_{soil}, k_{OH}) are determined instantaneously for each month given the geographic distribution of degradation rate constants for that month. The degradation rate constants are not geographically constant and vary monthly. For the ocean, a 1° x1° grid of the ocean is used where the temperature and salinity determine the chemical loss rate constant, wind speeds determine gas exchange coefficients, and biological degradation rate constants based on the field measurements of biological degradation are applied (Butler, 1994; Yvon and Butler, 1996; Yvon-Lewis and

Butler, 1997; Yvon-Lewis and Butler, 2002; Yvon-Lewis *et al.*, 2009; Hu *et al.*, 2012, 2013). Especially for the soil and oceanic uptakes, the uncertainties due to the extrapolation of spot measurements to global uptake rates and in the case of the oceanic uptake the calculation of the air-sea-exchange coefficients are significant sources of uncertainties. The Henry's law coefficients that describe the equilibrium between concentrations in the liquid phase and the gas phase are smaller sources of uncertainties. Loss due to reaction with OH has a pseudo first order rate constant defined as k[OH] which varies by latitude and month (Atkinson *et al.*, 2006; Spivakovsky, 2000). The total loss rate is then averaged globally for the final lifetime calculation (Yvon-Lewis and Butler, 2002; Yvon-Lewis *et al.*, 2009; Hu *et al.*, 2012, 2013). For CH_3Br and CH_3Cl, a 1° x1° grid of soil biomes is used, and a degradation rate constant for that biome is applied according to time of year which indicates if the biome is considered frozen, snow covered or exposed (Yvon-Lewis and Butler, 2002; Yvon-Lewis *et al.*, 2009; Hu *et al.*, 2012, 2013). For CCl_4, the soil uptake rate constant is from other published soil uptake rates and the atmospheric burdens used with those rates (Montzka and Reimann, 2011 and references therein). All of these distributions vary monthly, and we can determine the global loss rate constant for each month. The loss rate constants are averaged over the year grid cell by cell, and then determine a global annual loss rate constant (Yvon-Lewis and Butler, 2002; Yvon-Lewis *et al.*, 2009; Hu *et al.*, 2012, 2013). As no assumptions about an equilibrium between sinks and sources are made in these calculations, the results are transient lifetimes, but they are expected to be very good proxies for the steady-state lifetimes.

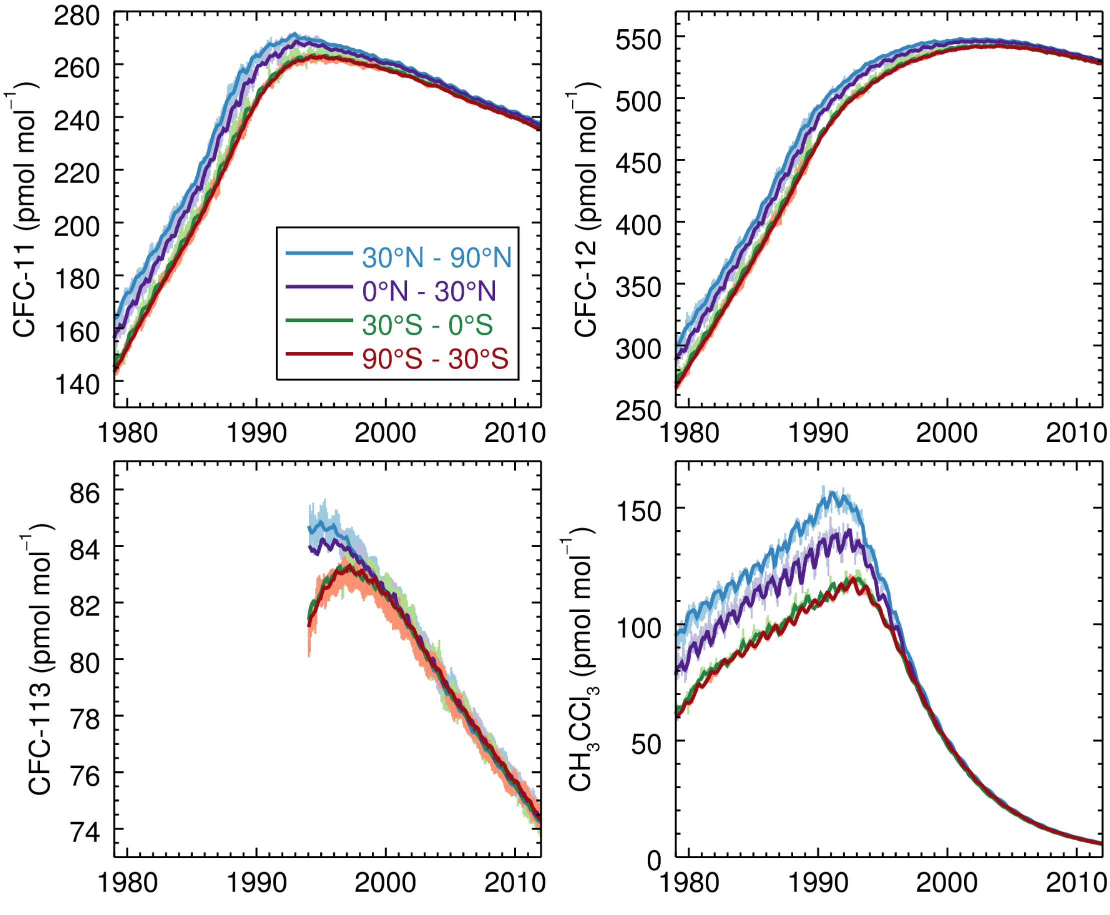

Figure 4.1. AGAGE measurements (shading), and optimized modeled mole fractions (solid lines) in the four surface semi-hemispheres for CFC-11, CFC-12, CFC-113 and CH_3CCl_3.

4.3.3.1 Methyl Bromide and Methyl Chloride

Atmospheric CH_3Cl and CH_3Br have many natural sources and sinks in common. Their common identified natural sources include the ocean, biomass burning, fungi, salt marshes, wetlands, rice paddies, mangroves and tropical rainforests (Hu *et al.,* 2010; Blei *et al.,* 2010; Yvon-Lewis *et al.,* 2009; Mead *et al.,* 2008a, b, Manley *et al.,* 2007; WMO, 2007, 2011; Lee-Taylor and Redeker, 2005; Dimmer *et al.,* 2001; Lee-Taylor and Holland, 2000; Rhew *et al.,* 2000; 2001; Rhew, 2011; Lobert *et al.,* 1999; Varner *et al.,* 1999; Watling and Harper, 1998; Moore *et al.,* 1996). Methyl bromide has the added anthropogenic source from fumigation uses (agricultural, structural and quarantine and pre-shipment (QPS)) (WMO, 2011). While the non-QPS anthropogenic emissions have been phased out as a result of the Montreal Protocol and its amendments, the QPS anthropogenic sources remain for CH_3Br.

Table 4.4. Published lifetimes of CH_3Br, CH_3Cl and CCl_4 from simple global box models. Numbers in parentheses are ranges reported in those studies.

Study	**Lifetime (years)**	**Type of Model**
Methyl Bromide		
Butler (1994)	1.2 (0.7-1.8)	Global box model
Yvon and Butler (1996)	0.8 (0.6-1.4)	Global box model
Yvon-Lewis and Butler (1997)	0.7 (0.6-0.9)	Global box model
Yokouchi *et al.* (2000)	1.0 (0.7-1.2)	Global box model
Hu *et al.* (2012)	0.8 (0.6-1.1)	Global box model
WMO (2011)	0.8	
Methyl Chloride		
Yvon-Lewis and Butler (2002)	1.3	Global box model
Xiao *et al.* (2010b)	1.0	(Inversion / Forward model)
Hu *et al.* (2013)	0.9 (0.7-1.1)	Global box model
WMO (2011)	1.0	
Carbon Tetrachloride		
WMO (1999)	35	
Yvon-Lewis and Butler (2002)	26	Global box model
WMO (2011)	20-30	(Adjustments to soil sinks and stratospheric lifetime)
WMO (2011)	26	
This Assessment	24 (19-40)	Global box model

Their shared identified sinks include degradation in the ocean, reaction with hydroxyl radicals (OH), photolysis in the stratosphere and uptake by soils (Butler, 1994; Yvon and Butler, 1996; Yvon-Lewis and Butler, 2002; WMO, 2003, 2007, 2011; Shorter *et al.,* 1995; Keene *et al.,* 1999; Keppler *et al.,* 2005). The total strength of known sinks outweighs the total strength of known sources by ~732 Gg yr^{-1} for CH_3Cl (Hu *et al.,* 2013) and ~35 Gg yr^{-1} for CH_3Br (WMO, 2011; Yvon-Lewis *et al.,* 2009). Forward models have been used to assess the strengths of these missing sources based on known sources and sinks (lifetimes).

Estimates of the budget and lifetime of CH_3Br have evolved over the years. In the early 1990s, when the oceans were first acknowledged as a sink for CH_3Br, Butler (1994) included oceanic uptake as an independent sink for CH_3Br in a box model reducing its estimated lifetime from 1.8 (Mellouki *et al.,* 1992) to 1.2 (0.7-1.8) years. Refinement of the oceanic sink and inclusion of a soil sink (Shorter *et al.,* 1995), further reduced the estimated lifetime to 0.8 (0.6-1.4) years (Yvon and Butler, 1996). In a subsequent update to this box model approach, biological degradation in the oceans (King and Saltzman, 1997) was included reducing the estimated lifetime further to about 0.7 (0.6-0.9) years.

Hu *et al.* (2012) revised the box model of Yvon-Lewis and Butler (2002) to include separate coastal and open ocean regions, a finer resolution ocean, revised flux parameterization and additional degradation rate constant measurements. This increased the estimate of the partial atmospheric lifetime with respect to oceanic loss from 1.8 (Yvon-Lewis and Butler, 1997) to 3.1 (2.3-5) years but did not change the overall atmospheric lifetime estimate, 0.8 (0.7-0.9) years.

While CH_3Cl is known to share some of the same sources and sinks as CH_3Br and supplies the most natural chlorine to the stratosphere, the box and forward modeling studies of it are fewer (Table 4.4). The lifetime as determined using the box model of Yvon-Lewis and Butler (2002) was 1.3 years. The combined inversion and forward modeling of Xiao *et al.* (2010b) produced a lifetime estimate of 1.0 years which is in agreement with the recommendations given in WMO (2011) and WMO (2007). Hu *et al.* (2013) revised the box model of Yvon-Lewis and Butler (2002) to include separate coastal and open ocean regions, a finer resolution ocean, revised flux parameterization and revised solubility to improve the estimate of the partial atmospheric lifetime with respect to oceanic loss which reduced the atmospheric lifetime estimate to 1.2 years.

While there have been some variations in the predicted lifetimes of CH_3Cl and CH_3Br, the best estimates are 1.2 (0.7-1.3, 2 σ) years for CH_3Cl and 0.8 (0.6-1.1, 2 σ) years for CH_3Br.

4.3.3.2 Carbon Tetrachloride

The global box models applied here do not require source information, only sinks, to estimate atmospheric lifetimes and partial atmospheric lifetimes. The sinks for CCl_4 include loss in the stratosphere, degradation in the oceans (Butler *et al.*, 2011; Yvon-Lewis and Butler, 2002; Lee *et al.*, 1999; Krysell *et al.*, 1994) and degradation in soils (Rhew *et al.*, 2008; Liu, 2006; Happell and Roche, 2003). In Montzka and Reimann (2011), the partial atmospheric lifetime with respect to stratospheric loss "was taken to be 35 yr based on previous modeling and observational work". This stratospheric lifetime was quoted relative to a CFC-11 stratospheric lifetime of 45 years (see discussion in section 4.4.). A best estimate of the stratospheric loss lifetime for CCl_4 including the results of Laube *et al.* (2013*)* and Volk *et al.* (1997) is 42 years (this chapter, Section 4.4.4). Happell and Roche (2003) estimated a partial atmospheric lifetime with respect to a soil sink of 90 (50-418, 1 σ) years. As discussed in Montzka and Reimann (2011), the results of Rhew *et al.* (2008) and Liu (2006) indicate that the rate constants for the uptake by some biomes included in the Happell and Roche (2003) calculation were too large by a factor of 2. The revised soil sink partial lifetime is approximately 195 (108-907, 1 σ) years (Montzka and Reimann, 2011). The oceanic loss rate constant used in the model to determine the partial atmospheric lifetime with respect to oceanic loss is estimated based on observations of oceanic surface water undersaturations. The partial lifetime with respect to oceanic uptake was determined to be 94 (82-191, 1 σ) years (Yvon-Lewis and Butler, 2002) based on the cruise data available at the time. Using additional cruise data, Butler *et al.* (2011) revised the partial lifetime with respect to oceanic loss to 81 (71-167, 1 σ) years. Using this revised oceanic uptake along with the new best estimate for stratospheric loss of 42 years (31-59 years, 2 σ; cf. Section 4.4.4) and the soil sink of 195 years results in an estimated transient lifetime of 24 (18-40, 2 σ) years. This estimate is slightly smaller than previous estimates discussed in Montzka and Reimann

(2011) of 26 (23-33 years, 1 σ). As discussed in Montzka and Reimann (2011), a faster decline in atmospheric mixing ratios than shown in observations would be expected based on this lifetime and the estimated bottom-up emission. This discrepancy cannot be resolved by this new estimate of atmospheric lifetime of CCl_4.

4.3.4 Global Satellite Measurements and Modeled Loss Rates

The study of N_2O by Johnston *et al.* (1979) was one of the first to use global measurements in combination with modeled photolytic loss rates to examine the distribution of stratospheric loss for a long-lived gas, and to assess its transient lifetime. This work employed a global N_2O climatology built on a number of aircraft, balloon, and rocket measurements of stratospheric vertical profiles that spanned a range of latitudes. One aspect of this approach, in comparison with lifetimes based on 2- or 3-D model simulations, is that the trace-gas distribution was specified. This eliminated the need for a detailed analysis of winds, mixing, and dynamical parameterizations, and the calculated loss does not involve uncertainties associated with trace-gas transport

Later studies by Crutzen and Schmailzl (1983); Ko *et al.* (1991); and Minschwaner *et al.* (1993) incorporated the use of global N_2O data from the stratospheric and mesospheric sounder (SAMS) instrument on the Nimbus 7 satellite. The availability of higher precision global data and a wider array of species from the UARS mission led to revised estimates of stratospheric loss of both N_2O and CFC-12 (Minschwaner *et al.,* 1998), and estimated global steady-state lifetimes of 117 ± 26 (1 σ) years (N_2O) and 103 ± 25 (1-σ) years (CFC-12). In this section, new results are presented using this technique (Minschwaner *et al.,* 2013) with global CFC-11 and CFC-12 distributions determined from MIPAS, ACE, CRISTA-1 and CRISTA-2, and CLAES satellite measurements discussed in Section 4.2.2.2.

The transient lifetime for CFC-11 was calculated from its global atmospheric burden, *B*, divided by its global loss rate, *L*

$$T(t) = \frac{B(t)}{L(t)} \tag{4.1}$$

where both *B* and *L* are determined from the local concentrations $n(\phi,z,t)$, photolysis rates $J(\phi,z,t)$, and reaction rates with excited state atomic oxygen $k_1[O(^1D)]$

$$B(t) = 2\pi\, R_E^2 \int dz \int n(\varphi,z,t)\cos\varphi\, d\varphi \tag{4.2}$$

$$L(t) = 2\pi\, R_E^2 \int dz \int n(\varphi,z,t)\left\{\mathrm{J}(\varphi,z,t) + \ k_1[\mathrm{O}(^1\mathrm{D})(\varphi,z,t)]\right\}\cos\varphi\, d\varphi \tag{4.3}$$

The above integrals are over altitude *z* and latitude ϕ (assuming zonal symmetry in the distribution and loss), and R_E is the Earth's radius.

As discussed above, the latitude and altitude distributions of CFC-11 and CFC-12 in Equations (4.2) and (4.3) are constrained from measurements. Results here involve global satellite observations from the following instruments: CFC-12 from CLAES between March 1992 and January 1993 (Nightingale *et al.,* 1996), CFC-11 from CRISTA-1 in November 1994 (Riese *et al.,* 1999) and from CRISTA-2 in August 1997 (Kuell *et al.,* 2005), CFC-11 from MIPAS between July 2002 and March 2004, CFC-12 from MIPAS between December 2002 and February 2003 (Hoffmann *et al.,* 2005, 2008), and both CFC molecules from ACE over the period 2006-2010 (Bernath *et al.,* 2005; Brown *et al.,* 2011). As shown below, the critical region where maximum calculated loss occurs for both CFCs is between 20 and 35 km altitude at low (+-30^o) latitudes (Figure 4.3).

Zonal averages for all three data sets were linearly interpolated onto a 1-km altitude grid from the surface to 50 km, and into latitudinal bins on a 5^o grid from 85°S to 85°N. Mole fractions above the top of vertical profiles were extrapolated to zero using cubic splines with matching gradients to the data at the uppermost valid measurement. Uncertainties in this extrapolation contribute to the overall uncertainty in lifetimes discussed below, although the magnitude of this error is small (<5%) in comparison with other uncertainties. At the bottom of vertical profiles, mole fractions extending down to 10 km altitude were linearly extrapolated where necessary up to the global/annual mean, tropospheric mole fraction at the time of each measurement (WMO, 2011). Mole fractions from 10 km to the surface were held constant at the 10-km value.

For CLAES CFC-12 and MIPAS CFC-11, mean seasonal distributions were constructed based on climatologies for four seasons: December-February, March-May, June-August, and September-November. The MIPAS CFC distributions incorporated adjustments to the altitude scale given in Hoffmann *et al.* (2008) by calculating geopotential heights using the native pressure grid from the MIPAS retrievals along with the temperature climatology discussed below. Corrections to the published altitudes were less than +0.5 km below 18 km, and between -0.2 and -1.8 km at higher altitudes. Global fields for ACE CFCs were constructed using one year of data in order to produce annual means with sufficient low latitude coverage. The MIPAS CFC-12 distribution is a mean over the months of December-February. For CRISTA-1 and 2 CFC-11, the data were assumed to represent means over +-70^o latitude for the months of November and August, respectively.

Figure 4.2 shows the MIPAS CFC-11 mean distribution for 2002-2004 along with the ACE annual mean 2008 climatology. Tropospheric levels of CFC-11 declined over the time between measurements by about 4%, which produces differences too small to be discerned in this figure and no corrections have been applied to account for such changes in the figure. The general stratospheric mole fraction patterns are similar for both distributions. The largest fractional differences between MIPAS and ACE occur at high latitudes below about 25 km altitude, although due to the pattern of loss presented below, such differences are not important for the CFC-11 lifetime. Above 20 km, MIPAS mole fractions are larger than ACE by 10-20% at all latitudes, and this difference is particularly conspicuous at low latitudes. Although smaller mole fractions in this region make it difficult to clearly see these differences in Figure 4.2, they do have a significant impact on the calculated lifetimes.

Photolysis frequencies (J-values) for CFC-11 and CFC-12 were calculated for each season, latitude, and altitude using the ultraviolet radiative transfer code described by Minschwaner *et al.* (1993). CFC absorption cross sections and the rate constants, k_1, for reactions with O(^{1}D) were taken from the recommendations of Chapter 3 in this assessment. Effects of Lyman alpha photolysis near 121 nm were not considered due to its negligible contribution to overall photodissociation of CFC-11 and CFC-12 (discussed in Chapter 3). The distributions of O(^{1}D) were modeled using steady-state photochemistry and calculated ozone photolysis frequencies. Climatologies of ozone (for UV opacity and for O(^{1}D)) and temperature (for incorporating temperature dependencies of reaction rates and cross sections) were adopted from the UARS zonal means developed by Minschwaner *et al.* (1998). Comparisons between this ozone climatology and others derived from UARS instruments (Wang *et al.,* 1999; Grooß and Russell 2005) indicated a small bias of +3% in the low-latitude stratosphere in the Minschwaner *et al.* (1998) climatology, and ozone concentrations were decreased uniformly by 3% for these calculations. Solar irradiances in the wavelength range from 115 to 420 nm were specified from measurements during March 2004 from the Solar Radiation and Climate Experiment (SORCE) (Rottman *et al.,* 2006). For more details of the cross sections and photolysis calculations, see Minschwaner *et al.* (2013).

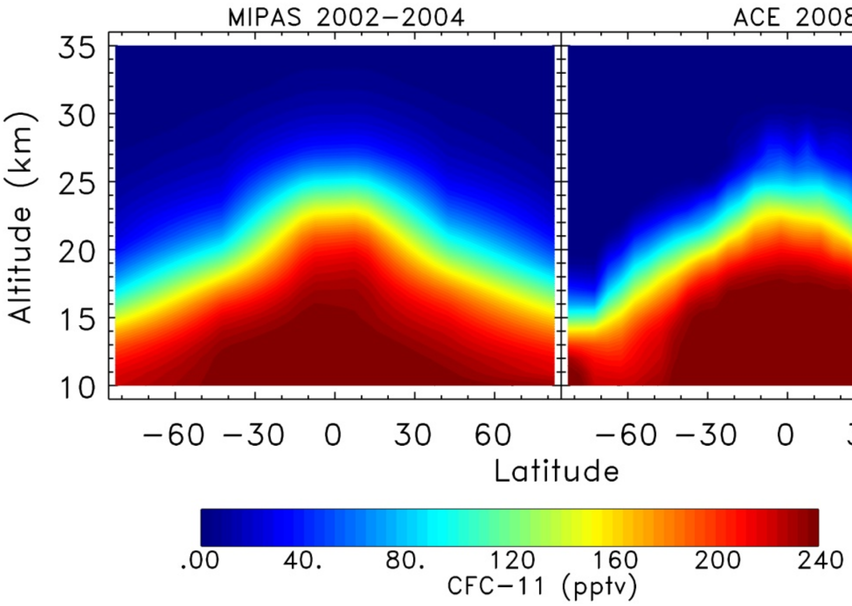

Figure 4.2. Zonal mean distributions of CFC-11 from MIPAS averaged over 2002-2004 (left), and from ACE for the 2008 mean (right).

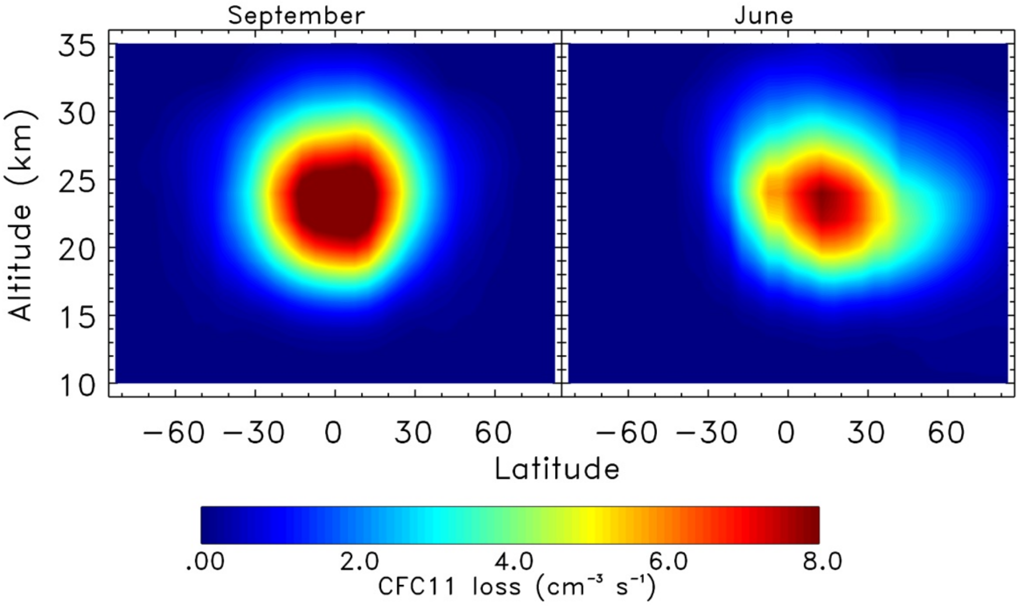

Figure 4.3. Loss rate for CFC-11 based on MIPAS distributions for September (left) and for June (right), in units of molecules cm^{-3} s^{-1}.

Calculated rates for stratospheric loss using MIPAS data are shown in Figure 4.3. Consistent with previous observationally based studies (Minschwaner *et al.,* 1993) and model results (Douglass *et al.,* 2008), CFC-11 loss is largest in the low latitude stratosphere between 20 and 28 km altitude. Globally integrated rates were found to be dependent on season; average removal rates are 12% larger during the equinoxes as compared to the solstices. These higher rates are primarily related to smaller solar zenith angles at low latitudes during equinox, with associated increases in actinic fluxes in the low latitude stratosphere where CFC-11 mole fractions are largest due to upwelling in the Brewer-Dobson circulation. An additional influence results from seasonal variations in ozone, with mole fractions slightly smaller in March than in June, which leads to greater penetration of solar radiation in March. Finally, there are seasonal changes in the MIPAS CFC-11 mole fractions that have about a 4% effect, although these act to oppose the impact of changes in actinic flux. For a fixed CFC-11 distribution, seasonal actinic flux and ozone changes produce larger variations of up to 16% in global loss rates.

The distribution of CFC-12 loss (not shown) also shows largest rates in the tropical stratosphere, but CFC-12 destruction is shifted upward about 6 km relative to CFC-11. Also, CFC-12 loss rates are 30-40% smaller than for CFC-11, which along with a larger global burden, translates to a longer lifetime for CFC-12 compared with CFC-11.

For both CFCs, the reaction $O(^1D)$ accounts for 4-8% of the total loss in the tropical stratosphere between 20 and 35 km. This reaction does become important to the destruction rate below 12 km and in the lower stratosphere at high latitudes, but these regions have a negligible impact on the global loss. Thus, the global sink for both CFCs is governed primarily by direct photodissociation.

Table 4.5 lists the sources of CFC-11 data and observation time periods used in this analysis, the global mean loss rates and burdens, and the transient and steady-state lifetimes derived from the measurements. All loss rates and burdens are based on calculated means over four seasonal values, with both CRISTA CFC-11 distributions held fixed and ACE values based on 4-year averages of the computed annual means. Table 4.5 also provides uncertainties in steady-state lifetimes based on an analysis of multiple sources of error and standard error propagation methods (Minschwaner *et al.,* 2013) applied to estimated 2σ uncertainties. The average fractional error in lifetime from a single dataset is about 55%. Uncertainties associated with CFC climatologies (33-41%) and with oxygen opacity between 185 and 220 nm (34% on photolysis loss) account for most of the uncertainty in lifetimes. Other primary sources of uncertainty are due to ozone opacity (16%) and CFC absorption cross sections (28% for CFC-11 and 14% for CFC-12 at the relevant stratospheric temperatures).

The steady-state lifetime of a long-lived gas, where emissions to the atmosphere exactly balance photochemical loss, will be different from its instantaneous lifetime if the mean tropospheric concentration is changing with time (which implies an imbalance between sources and sinks). This difference is due to the finite time lag between temporal changes in abundances for the stratosphere relative to the troposphere. For CFC-11, decreases in global mean tropospheric abundances during 1997-2010 were between -0.8%/yr and 1%/yr, indicating a larger stratospheric loss relative to tropospheric emissions. Assuming a mean time lag of 2 years for air to ascend through the tropical tropopause to 30 km altitude (Schoeberl *et al.,* 2008), steady-state lifetimes are 1.6% to 2% longer than transient lifetimes for the CRISTA-2, MIPAS, and ACE distributions. For CRISTA-1, 1994 marks the approximate peak in tropospheric mole fraction and therefore the steady-state lifetime is nearly identical to the computed transient lifetime.

Table 4.5. Summary of CFC-11 lifetimes from satellite observations. While CRISTA-1 and CRISTA-2 are listed separately, they have been combined to one value for the calculation of the mean. All uncertainties given in this table represent 2σ ranges.

Instrument	**Observation Period Used**	**Mean Global Burden (10^{34} molecules)**	**Mean Loss Rate (10^{25} molecules s^{-1})**	**Transient Lifetime (yr)**	**Steady-State Lifetime (yr)**
CRISTA-1	Nov 1994	2.71	1.63	52.7	52.9 (33-140)
CRISTA-2	Aug 1997	2.64	1.39	60.0	60.7 (37-161)
MIPAS	2002-2004	2.50	2.24	35.4	36.1 (23-84)
ACE	2006-2010	2.38	1.67	45.2	46.1 (29-121)
Best Estimate					44.7 (30-91)

The multi-instrument mean CFC-11 steady-state lifetime is 44.7 (30-91) yr. The mean value is determined by an equal-weighted mean of the inverse lifetimes (as these, contrary to the lifetimes, exhibit symmetric uncertainties) based on CRISTA, MIPAS, and ACE datasets. Since the CRISTA-1 and CRISTA-2 data are from the same instrument with only minor differences in calibration and processing, the CRISTA results are not completely independent and are averaged first, before computing the multi-instrument mean that includes MIPAS and ACE results. Given the large number of tropical profiles from each dataset, differences in statistical errors between the three datasets are negligible. However, data that cover less than one month (CRISTA-1 and CRISTA-2) may be biased by seasonal changes in tropical CFC-11 profiles, which is estimated from MIPAS data to impact the derived lifetime by about 4%. A weighted mean lifetime that accounts for effects of this magnitude in the CRISTA datasets is shorter than the arithmetic mean by only 0.3 yr, thus an equal weighting is applied to the three datasets in computing the multi-instrument mean.

The large spread in CFC-11 lifetime derived from the four measurements (24.6 yr from minimum to maximum) results primarily from differences in low latitude mole fractions between 20 and 28 km altitude. This range in lifetime is also consistent with the estimated uncertainties due to stratospheric concentrations (33-41%). For the purposes of comparison, mean tropical profiles can be scaled to match tropospheric mole fractions for 1994, near the peak period of CFC-11 loading. Resulting differences between data sets are fairly large at 25 km, with the smallest mole fraction of 56 pmol mol^{-1} from CRISTA-2 and the largest of 100 pmol $mol^{-1}$from MIPAS. This broad range is reflected in the derived CFC-11 steady-state lifetimes, from 60.7 yr for the CRISTA-2 climatology, to 36.1 yr for the MIPAS climatology.

Table 4.6 lists the CFC-12 loss rates, burdens, and lifetimes derived from the three sets of measurements. CFC-12 abundances in the troposphere peaked around 2002-2003, and growth rates of +2.5%/yr for CLAES, zero for MIPAS, and -0.5%/yr for ACE have been adopted. Coupled with a mean age at 30-35 km in the tropics of 2.5 years, these growth rates were used to derive the steady-state lifetimes shown in Table 4.6. As indicated in the table, the variation between data sets for the CFC-12 steady-state lifetime is much smaller than for CFC-11, with a max-min spread of only 3.5 yr. This level of agreement may be fortuitous given the 2-σ uncertainties of 32-51% due to stratospheric profile error sources. It should be noted that the reanalysis of CLAES CFC-12 data presented here includes revisions to the absorption cross section and ozone opacity in comparison to Minschwaner *et al.* (1998), leading to a small difference of about 3 yr in the derived lifetime. The multi-instrument mean CFC-12 steady-state lifetime (determined again as equal-weighted mean of the inverse lifetimes) is 106.6 (79-166) yr.

Table 4.6. Summary of CFC-12 lifetimes from satellite observations.

Instrument	**Observation Period Used**	**Mean Global Burden (10^{34} molecules)**	**Mean Loss Rate (10^{25} molecules s^{-1})**	**Transient Lifetime (yr)**	**Steady-State Lifetime (yr)**
CLAES	1992-1993	5.00	1.40	113.3	108.0 (76-185)
MIPAS	2002-2003	5.50	1.62	107.5	107.5 (69-250)
ACE	2006-2010	5.31	1.63	103.3	104.5 (71-201)
Best Estimate					106.6 (79-166)

Mean, steady-state lifetimes derived here 44.7 (30-91) yr for CFC-11 and 106.6 (79-166) yr for CFC-12) are in excellent agreement with the most recent WMO Ozone Assessment recommendations (45 yr for CFC-11 and 100 yr for CFC-12) (WMO, 2011). They deviate from the latter by only 1% and 7% for CFC-11 and CFC-12, respectively, i.e., much less than their uncertainties. The primary differences between CFC-11 and CFC-12 lifetimes in this analysis arise from differences in the absorption cross sections, which impact photolysis rates in Equation (4.3), and from differences in stratospheric vertical profiles, mainly within the tropical stratosphere below 35 km altitude. A major difficulty in calculating CFC-11 destruction relates to the very large vertical gradient in mole fraction. This large gradient complicates space-based observations that may have extended vertical fields of view, averaging kernels, or uncertainties in absolute altitude registration, and small errors in any of these quantities are magnified in calculated CFC-11 loss rates.

Loss rate calculations were also conducted using CFC-11 vertical profiles from model simulations of the GEOSCCM (see Chapter 5), using zonal and annual mean model outputs for 1997 and 2007. Table 4.7 compares CFC-11 global mean loss rates, burdens, and lifetimes. Differences between transient lifetimes calculated here and those based on model results range between 3 to 5%, with model lifetimes systematically longer by about 2 to 3 yr. These differences result from offsets in the calculations of global burdens (1-2%), and in global loss (2-3%). For global burdens, differences are likely related to longitudinal variations in tropospheric mole fraction and temperature (density) fields, since model CFC-11 burdens calculated using zonal mean fields produce nearly identical burdens as those for the satellite observation method shown in Table 4.7. However, modeled loss rates are unchanged between the 3-D and zonal mean cases, which suggests that loss rate differences shown in the table are more likely related to systematic differences in tropical ozone climatologies or in the treatment of oxygen opacity. In general, however, the level agreement in CFC-11 lifetimes from both methods is well within the magnitude of uncertainties noted previously in Table 4.5.

Table 4.7. Comparison of CFC-11 lifetime calculations. Sat Obs. Method refers to the calculation methods described in this section.

Method	Observation Period Used	Mean Global Burden (10^{34} molecules)	Mean Loss Rate (10^{25} molecules s^{-1})	Transient Lifetime (yr)
Sat Obs. Method	1997 mean	2.63	1.62	51.6
GEOSCCM	1997 mean	2.61	1.52	54.7
Sat Obs. Method	2007 mean	2.45	1.57	49.4
GEOSCCM	2007 mean	2.43	1.48	52.0

4.4 Lifetimes Derived from Stratospheric Tracer-Tracer Correlations

4.4.1 The Methods and Their Applicability

Tracer-tracer relations and tracer-mean age relations can be used to derive stratospheric lifetimes (which are equivalent to atmospheric lifetimes for 7 out of the 30 species mentioned in Table 4.1), i.e., the CFCs and Halon-1301; for Halon-1202 tropospheric loss is dominant and for Halon-1211 and 2402 tropospheric and stratospheric lifetimes are on the same order of magnitude (see e.g., Newland *et al.*, 2012 and references therein). The applicability of this approach is discussed in Chapter 2 from a theoretical point of view. Due to theoretical considerations, these methods require the tracer-tracer or tracer-mean-age slopes at the extratropical tropopause, best taken during the winter half year that dominates net transport (Plumb, 1996). From a practical point of view, the slope at the end point of the correlation curve can be difficult to measure and may be affected to some extent by variability of upper tropospheric tracer distributions and of cross-tropopause transport. These effects are likely to be small for correlations between two long-lived tracers (relative method), but may become more problematic for the (absolute) age-tracer method proposed by Volk *et al.* (1997), as age-tracers like SF_6 and CO_2 are not sufficiently well mixed in the troposphere. Even without these potential caveats, uncertainties of lifetimes derived from the absolute method are considerably larger than for the relative method (Volk *et al.,* 1997). Therefore, values derived with the absolute method will not be considered in this assessment report. The reader is referred to Chapter 2 for further discussion of the applicability of this method.

The tracer-tracer method (Plumb and Ko, 1992; Plumb, 1996) relates the slope of the relation between two long-lived tracers, χ_1 and χ_2, to the ratio of their respective fluxes through the tropopause (equaling their stratospheric sinks) and thus to the ratio of their stratospheric lifetimes:

$$\frac{\tau_1}{\tau_2} \cong \frac{d\chi_2 B_1}{d\chi_1 B_2}$$

where B_1 and B_2 are the global atmospheric burdens of the two tracers. As tracer-tracer relations are generally non-linear in the lower stratosphere, the accurate derivation of the slopes at the extratropical tropopause end-point of the relation presents a major challenge in applying either method. Using near-global high-resolution aircraft data from the 1994 ASHOE/MAESA campaign, Volk *et al.* (1997) found the following measures to be essential to derive consistent slopes with transparent uncertainty estimates: (i) observations below the tropopause have to be excluded as spatial and temporal tropospheric variations result in tracer relations that are unrelated to τ, and (ii) an error-weighted orthogonal fitting routine has to be used in order to eliminate sensitivity of the slopes to switching X and Y axis. They then measured the slopes locally along the tracer relation (over tracer intervals corresponding to 2 years of age) and extrapolated these local (linear) slope results to the tropopause end point of the relation using a quadratic fit over a tracer interval corresponding to about 3 years of age. This procedure thus relies less on local information at the tropopause itself, where variations driven by tropospheric sources and transport (including seasonal variations) may become significant, but makes use of information across a major part of the lower stratosphere that is responsible for establishing the relation between the tracer fluxes and the tracer slopes; in addition the 3-year age range used for the final extrapolation also effectively averages over seasonal variations in stratospheric transport. Errors propagated through the complete procedure resulted in 1-σ uncertainties of the derived slopes at the tropopause of 5-10% for the tracer-tracer method.

A further obstacle in deducing lifetimes with this method is that most of the species involved have temporal trends in their atmospheric mole fractions. The slope is thus determined by a combination of chemical decay and temporal trends that need to be separated from each other. A method how to take these trends into account has been proposed by Volk *et al.* (1997) and was applied to the ASHOE/MAESA observations. A further method to detrend stratospheric observations, based on the knowledge of the tropospheric trend and the mean age of air has been suggested based on model work (Plumb *et al.,* 1999). One limitation of this latter approach is, however, that it relies on model calculations of the age spectrum and the chemical breakdown of trace gases in the stratosphere. While – in contrast to the method suggested by Volk *et al.* (1997) - this method would allow combining observations from different years, the associated uncertainties are expected to be rather high.

In this section, we will thus focus on investigations using the method suggested by Volk *et al.* (1997) that relies on determining a correction factor for the specific time of the measurements. The theoretical as well as the practical derivation of the correction factor is somewhat complex. In brief it makes use of (i) the observed tracer gradient with respect to age at the tropopause $d\chi/d\Gamma$, (ii) a quadratic fit to the non-linear time series of tropospheric mole fractions of the respective species during a 5-year period prior to the stratospheric observations, and (iii) a model-estimate of the width Δ of the stratospheric age spectrum (Hall and Plumb, 1994) relative to the mean age, i.e., the parameter Δ^2/Γ, which is roughly constant over the lower stratosphere according to three-dimensional (3-D) transport models. The growth correction factors C become particularly large for species that are very long-lived or for species that exhibit strongly non-linear growth, with the largest factors (in 1994) for CFC-113 (C=0.65+/-0.12) and CFC-12 (C=0.77+/-0.07). Results for the lifetimes using the relative method derived by Volk *et al.* (1997) are discussed in Sections 4.4.2 and 4.4.3, and are listed in Table 4.8 together with new results based on more recent observations (Laube *et al.,* 2013; Brown *et al.,* 2013).

4.4.2 Lifetime Estimates from *In Situ* Data

Only a few of the publications mentioned in Section 4.2.2 use *in situ* measurements to estimate stratospheric lifetimes. Exclusion of studies with limited precisions and thus comparably high uncertainties (Kaye *et al.,* 1994; Avallone and Prather, 1997) reduces the number of studies. The most extensive evaluation is presented in Volk *et al.* (1997). All other studies rely to a large part on the methods developed in this work. The studies of Bujok *et al.,* 2001 and Laube *et al.,* 2010b focus on individual molecules only and estimate stratospheric lifetimes from correlation slopes against CFC-11 using the WMO reference lifetime of 45 years. Bujok *et al.,* 2001 derive an N_2O lifetime of 91±15 years, which is considerably lower than the 121±14 years estimated by Volk *et al.,* 1997 (based on 45 yr for CFC-11). Laube *et al.,* 2010b estimated the lifetime of HFC-227ea to be 370 years. However, this latter estimate revealed one of the limitations of the tracer-tracer correlation method. Very long stratospheric lifetimes result in correlation slopes close to zero, so that even small variations result in large uncertainty ranges (270 to 840 years in the case of HFC-227ea). The applicability of this method is thus currently very limited for several compounds of interest in this report, namely CFC-114, CFC-115, and HFC-23. Finally, the most recent work is that of Laube *et al.* (2013). Laube *et al.* (2013) combine *in situ* observations from the Geophysica aircraft and from balloons to derive burdens and tracer-tracer correlations. Ratios and their 2-σ uncertainty ranges of stratospheric lifetimes relative to CFC-11 derived from these studies are given in Table 4.8 along with the numbers recommended in the latest WMO Ozone Assessment (WMO, 2011) and results from the satellite-based study of Brown *et al.* (2013) discussed in the following section. We note that within the given 2-σ uncertainties (in most cases even within 1 σ), all values of the *in situ* studies agree with each other and with the values from WMO (2011).

Table 4.8. Overview of stratospheric lifetime ratios relative to CFC-11 and a combined best estimate (based on error weighted means) compared to those recommended in the most recent WMO Ozone Assessment (WMO, 2011) and (for N_2O) the IPCC Assessment (IPCC, 2007). Ranges indicate 2-σ uncertainties (the symmetric errors given in the original work by Volk *et al.* (1997) have been converted to asymmetric errors more accurately representing 2-σ uncertainties.)

	Volk *et al.,* 1997	**Laube *et al.,* 2013**	**Bujok *et al.,* 2001**	**Brown *et al.,* 2013**	**Best estimate**	**WMO 2011** **[a] IPCC 2007**
Trace gas						
N_2O	2.70(2.18-3.54)		2.02 ±0.22	2.74(1.52-14.03)	2.70(2.20-3.50)	2.53[a]
CH_4	2.06(1.70-2.62)			4.33(2.36-25.94)		
CFC-12	1.92(1.54-2.56)	1.66 (1.36-2.15)		2.5(1.73-4.49)	1.91(1.65-2.27)	2.22
CFC-113	2.24(1.44-5.02)	1.37 (1.12-1.77)			1.56(1.28-1.98)	1.89
CFC-11	1.00	1.00		1.00		
CCl_4	0.72(0.59-0.93)	0.87 (0.66-1.28)		0.77 (0.49-1.81)	0.78(0.66-0.94)	0.78
CH_3CCl_3	0.76(0.58-1.11)	0.50 (0.29-1.86)			0.74(0.57-1.04)	0.87
Halon-1211	0.52(0.38-0.85)	0.61 (0.48-0.81)			0.58 (0.48-0.74)	
Halon-1301		1.37 (1.13-1.74)			1.37 (1.13-1.74)	1.44
HCFC-22		3.06 (1.31-∞)			3.06 (1.31-∞)	4.13
HCFC-141b		2.02 (0.82-∞)			2.02 (0.82-∞)	1.44
HCFC-142b		6.75 (1.39-∞)			6.75 (1.39-∞)	3.56
CH_3Cl				1.54 (0.53-∞)	1.54 (0.53-∞)	

4.4.3 Lifetime Estimates from Satellite Data

ACE-FTS satellite measurements from 2005 to 2010 have been used to calculate steady-state stratospheric lifetime ratios of CFC-12, CCl_4, CH_3Cl, N_2O and CH_4 relative to CFC-11 using the method described by Volk *et al.* (1997); (Brown *et al.,* 2013).

The data were divided into occultations made during stratospheric summer and winter from the Northern and Southern Hemispheres. Data were selected between 30^0 N/S and 70^0 N/S. These latitude bands were chosen so that data inside the polar vortex and the tropics would not be included. The data were separated using the following criteria: Northern Hemisphere Summer (May* – June – July – August – September – October*); Northern Hemisphere Winter (November – December – January – February – March – April); Southern Hemisphere Summer (November* – December – January – February – March – April*); and Southern Hemisphere Winter (May – June – July – August – September – October). [We note that months marked with * have been selected to increase the amount of data used in this study despite not being true stratospheric summer months.] These data were also divided by year, which produces 24 different data bins.

Mean correlation profiles were calculated using the mean mole fractions of both the correlating species (for example CFC-12) and CFC-11 calculated every 2 pmol mol^{-1} in the mole fraction of CFC-11. The error of each point was calculated from the standard deviation of the data within this 2-pmol mol^{-1} window. The derivation of the correlation slopes at the tropopause then followed nearly exactly the procedures described in Volk *et al.* (1997). First, the slope of the data in a window with width of 80 pmol mol^{-1} (of CFC-11) was calculated every 5 pmol mol^{-1} of CFC-11. A second-degree polynomial, weighted by the error of the points (1-σ error in the fit of the line), was then fit to the slope data and extrapolated to the tropopause using the VMR of CFC-11 retrieved by ACE-FTS at the tropopause. The tropopause slopes thus determined were corrected for the effects of tropospheric growth according to the method described in Volk *et al.* (1997) and outlined above (Section 4.4.1). The required slope of CFC-11 relative to the age of air at the tropopause was calculated from measurements made with instruments onboard the Geophysica aircraft in October 2009 and January 2010 by Laube *et al.* (2013). This value was scaled by the effective linear growth rate of CFC-11 between 2005 and 2010. Examples of the correlation plots produced in this study are presented in Figure 4.4.

An analysis of the altitude dependent systematic errors in ACE-FTS retrievals has not been carried out at this time. However, ACE-FTS occultations have been compared to data from other instruments such as the MK-IV and FIRS-2 balloon borne spectrometers (e.g., Mahieu *et al.,* 2008). Previous validation papers for N_2O, CH_4, CFC-11 and CFC-12 have not shown significant altitude dependent errors for the altitude range used in this study (Mahieu *et al.,* 2008; Velazco *et al.,* 2011). In addition to these comparisons, the profiles of CFC-11 and CFC-12 were compared to those from the SLIMCAT 3-D Chemical Transform Model (Brown *et al.,* 2011). The profiles used in this work showed that, whilst there were differences in the VMR from ACE-FTS and from SLIMCAT the overall shapes of the profiles were extremely similar. The differences between VMRs from ACE-FTS and other instruments (mentioned previously) can be used as a proxy for the systematic error, due to the fact that the full systematic errors associated with ACE-FTS retrievals are not known at this time. The methods described in this section were repeated using ACE-FTS VMR that were modified by the differences calculated in previous validation work. The values used to modify the VMRs were + 10% for CFC-11 and CFC-12 from the validation work of Mahieu *et al.* (2008). Work by Velazco *et al.* (2011) also showed differences of + 10% for CH_4 and N_2O. The results of the reanalysis using these errors were combined with the statistical error.

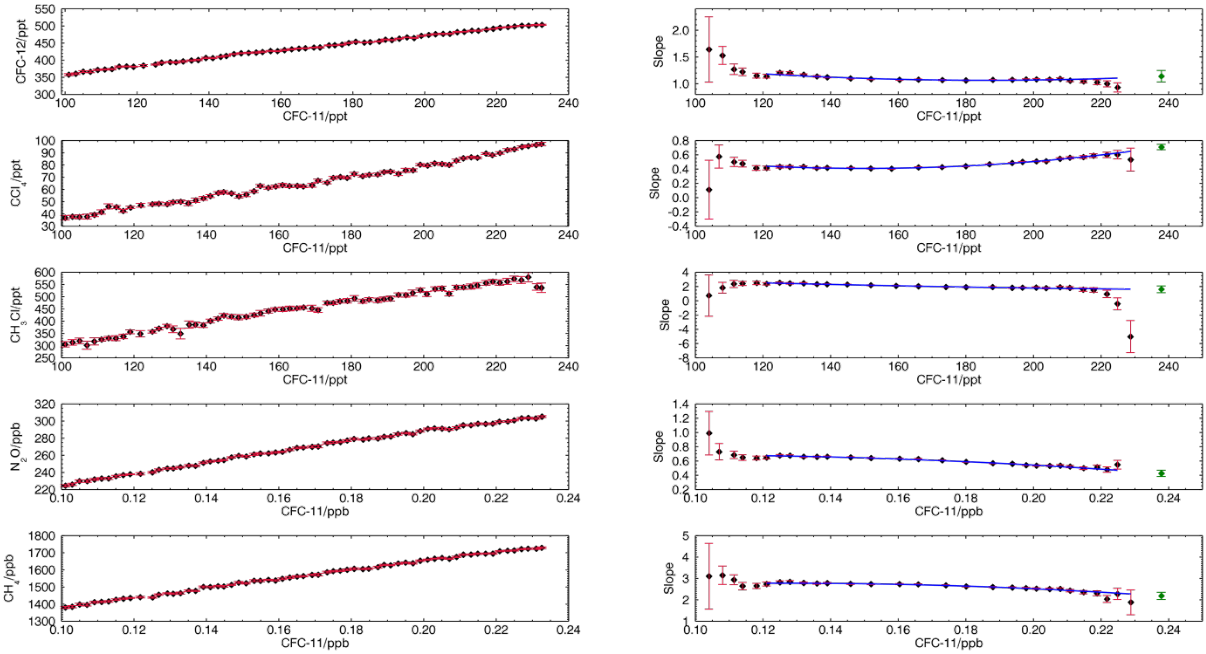

Figure 4.4. Correlations between the volume-mixing ratios of CFC-12, CCl_4, CH_4, CH_3Cl and N_2O and CFC-11 for the data from the Northern Hemisphere during the stratospheric winter of 2008. Left panels: The mean correlation curves. Each point represents the mean of the VMR, of both CFC-11 and CFC-12, in a window of 2 ppt of CFC-11. The error on these points is the standard deviation of the mean of the data within each 2 ppt window. Right panels: The local slope of data in an 80 ppt of CFC-11 window. The error on the points is the fitting error of this fit. The blue line is a second-degree polynomial fit to the local slopes. The green point is the extrapolated slope at the tropopause.

The remaining species, CH_3Cl and CCl_4, are more problematic than the other species. Previous validations of these species have shown large differences between ACE-FTS retrievals and the retrievals from other instruments. For example comparisons between ACE-FTS and the MK-IV instrument (Velazco *et al.,* 2011) found differences of 30% in the VMR retrievals of CH_3Cl. The errors on ACE-FTS retrievals of CCl_4 are estimated to be between 20 and 30% (Allen *et al.,* 2009). The estimation of systematic errors for the CCl_4 retrieval is complicated by the position of the spectral feature used to retrieve CCl_4 VMR. There is an interfering Q-branch of CO_2, the line mixing of which is not properly accounted for in the forward model. Similarly the Q-branch of CH_3Cl suffers from line mixing which is not properly included in the forward model. The effects of line mixing on both of these retrievals are most serious in the troposphere, where the density of the atmosphere is at its greatest. In the stratosphere, where the density of the atmosphere is lower, line mixing becomes less of a problem within the retrieval. Quantifying the effects of line mixing on the retrieved VMR is a research project in and of itself. In this work we have approximated the systematic errors to be - 30% for CH_3Cl (Velazco *et al.,* 2011) and + 20% for CCl_4 (Allen *et al.,* 2009). Once more lifetimes were calculated using VMR that had been modified by the corresponding systematic error. These errors represent the best attempt to quantify the effect of systematic errors on the lifetimes of CCl_4 and CH_3Cl; however, due to the reasons outlined previously these errors may be different to those quoted here.

The lifetime ratios calculated from the tracer correlations show considerable spread between the individual hemisphere/season/year bins that is sometimes larger than expected from the estimated uncertainties. However, there are no systematic (seasonal, interhemispheric) variations apparent. Therefore, the mean lifetime of each species relative to CFC-11 was determined from the individual bins as error-weighted average of the individual inverse lifetimes (a quantity with symmetric uncertainties). These ratios are listed in Table 4.8 along with the results of the *in situ* studies.

4.4.4 Best Estimate of Lifetime Ratios

There are two systematic studies on lifetime ratios based on *in situ* measurements (Volk *et al.,* 1997 and Laube *et al.,* 2013) and one that is based on satellite observations (Brown *et al.,* 2013). As the two latter studies closely follow the methods (and even in detail the practical procedures) described in Volk *et al.* (1997) and summarized in Section 4.4.1, the three studies can be considered very consistent with each other regarding their methodology. Although there are notable differences for some species between the ratios derived by these studies, we emphasize that the results do agree within their 2-σ error uncertainties (with the exception of CH_4). These three independent studies all have strengths and weaknesses. While the Volk *et al.* (1997) study was carried out when atmospheric trends for CFC-12 and CFC-113 were quite large, the study by Laube *et al.* (2013) is based on a much smaller data set and only covers one season, and the Brown *et al.* (2013) study is based on satellite data which may be more prone to systematic uncertainties than *in situ* data. We therefore decided to base our recommendation on an error-weighted average of the three ratios (where the mean was again calculated for the inverse lifetimes, which exhibit symmetric uncertainties). As noted above, these studies all agree within their combined estimated error, with the exception of the studies by Volk *et al.* (1997) and by Brown *et al.* (2013) for the stratospheric lifetime of methane. We thus give no recommendation of the stratospheric lifetime of CH_4, as one or both of the studies must have unaccounted errors for this species. All our best estimates for the ratios of stratospheric lifetimes relative to CFC-11 are given in Table 4.8. The implications and the recommendations for atmospheric lifetimes based on observations are drawn in the following Section 4.5.

4.5 Conclusions

In this chapter different methods are applied to derive lifetimes of atmospheric trace gases based on their measurements in the atmosphere. Some of these methods rely on a combination of modeling and observations (Section 4.3) while relative lifetimes of some species can be deduced from stratospheric correlations (Section 4.4) directly. While this latter approach does not require an atmospheric model, it does rely on a complex conceptual framework and must also be applied with care. Common to all of these techniques is the need for high precision, high accuracy, and long-term internally consistent data from both the troposphere and the stratosphere. We note that the absolute method to derive stratospheric lifetimes from correlations between the mole fraction of a trace gas and its mean age (Volk *et al.,* 1997) is not considered here due to the larger uncertainties associated to this method (see also discussion in Chapter 2). All methods applied here rely on data from different time periods. As even steady-state atmospheric lifetimes are not constant in time, but may change e.g., due to changing chemistry or changing dynamics, there may be both interannual variability and long-term changes in atmospheric lifetimes over the periods of investigations. However, the uncertainties in all the lifetimes derived here are significantly larger than any expected long-term changes, so we will assume in the following discussion that all values derived here can be compared and combined to yield best estimates.

As CFC-11 has traditionally been used as a reference species to derive lifetimes of other compounds, its stratospheric lifetime is of particularly high importance. WMO (1999) has recommended a change of the best estimate atmospheric lifetime from 50 years to 45 years based in part on values from inverse modeling (52 years, Cunnold *et al.,* 1997), from global loss calculated using balloon data (41.5 yr, Minschwaner *et al.,* 1993) and on the lifetime of 41±12 years derived from correlations between mean age and CFC-11 in the stratosphere (Volk *et al.,* 1997). New independent studies based on inverse modeling (Rigby *et al.,* 2013), comparable to the study of Cunnold *et al.* (1997) suggest a steady-state global CFC-11 lifetime of 53 (40-72, 2σ) years, averaged from inversions of AGAGE and NOAA data, respectively. The result is thus between current model estimates of 56 years (Douglass *et al.,* 2008) and the current WMO recommendation of 45 years. For CFC-12 Rigby *et al.* (2013) deduce a lifetimes of 111 (79-157, 2σ) years, again averaged from the inversions of AGAGE and NOAA data, respectively. The study by Rigby *et al.* (2013), while having significant uncertainties, suggests that the CFC-11 lifetime may be slightly longer than currently recommended, whereas the CFC-12 value of both studies, while being slightly higher than the WMO recommendation, is in good agreement with the current recommendation of 100 years. In the case of the inverse modeling improved independent estimates of emissions would allow to better constrain the lifetimes.

The second method used to derive global steady-state lifetimes of CFC-11 and CFC-12 is based on the combination of observed global distributions and calculated loss rates (Minschwaner *et al.,* 2013) and yields lifetimes of 45 (30-91, 2σ) years and 107 (79-166, 2σ) years for CFC-11 and CFC-12, respectively. This method relies on accurate information about the actinic flux, the temperature-dependent absorption cross section and the global distribution of the respective species, especially in the loss region. Due to the steeper gradient of the shorter-lived species CFC-11 in comparison to CFC-12, this method will work better for CFC-12 then for CFC-11. In order to reduce uncertainties in the future, better knowledge of actinic UV- fluxes in the tropical loss region, better information on absorption cross section and in particular for CFC-11 improved knowledge of the global distribution from well-validated satellite data with high vertical resolution are necessary.

Relative stratospheric lifetimes of two species can be derived based on the correlation observed between these species in the lower stratosphere. The results from such studies using both *in situ* and satellite data and the best estimate deduced from these studies are shown in Table 4.8. The currently recommended lifetimes of 100 years for CFC-12 and 45 years for CFC-11 would suggest a ratio of 2.22. This is in poor agreement with the results of the two *in situ* studies available (Volk *et al.,* 1997; and Laube *et al.,* 2013). Both these studies suggest that the ratio should be lower, i.e., 1.92 (1.54-2.56) (Volk *et al.,* 1997) and 1.66 (1.36-2.15) (Laube *et al.,* 2013). The ratio of 2.5 (1.73-4.49) based on satellite correlation studies (Brown *et al.,* 2013) is on the contrary higher than the WMO recommended lifetime ratio. Our best estimate of the lifetime-ratio between CFC-12 and CFC-11 is 1.91 (1.65-2.27). This ratio agrees with the ratio found from satellite observations and modeling of the loss rate (2.30) and from inverse modeling (2.08) within its 2σ range and within the combined 1σ ranges. Based on these ratios, we conclude that a lifetime of about 50 years for CFC-11 and 105 years for CFC-12 provides the best agreement with observational data and observation-based studies. Taking into account all information available, including model studies from Chapter 5, a global steady-state lifetime of 52.3 (43-67, 2σ "most likely range" estimate) years is derived (see Chapter 6).

In the case of CFC-11 it must further be taken into account that some loss also occurs in the troposphere (e.g., Minschwaner *et al.*, 2013, see also discussion in Chapter 5). Using the model-derived tropospheric lifetime of 1870 years, we derive a stratospheric steady-state lifetime of 53.8 (44.3-68.8, 2σ) years, on which we base the following discussion. The stratospheric lifetime of CFC-12 derived from this is 103 (81-140) years. All uncertainties given are 2-σ uncertainties unless noted otherwise. The values given here will thus differ from the absolute values given in the original publications. Table 4.9 summarizes estimates of global lifetimes and Table 4.10 those for stratospheric lifetimes based on the results discussed in this chapter.

Global lifetimes for CFC-113 of 109 (89-133) and 109 (86-140) years are derived from inverse modeling (Rigby *et al.,* 2013), which is longer than the currently recommended value of 85 years. The correlation studies yield a best-estimate ratio of 1.56 (1.28-1.98) for the lifetime of CFC-113 relative to CFC-11. A direct comparison of vertical profiles of CFC-12 and CFC-113 (Laube *et al.,* 2010a, 2013) and cross sections (Sander *et al.,* 2011) suggests that CFC-113 should be shorter lived than CFC-12, as also currently recommended by WMO. Based on a stratospheric lifetime of 53.8 years of CFC-11 we derive a stratospheric lifetime of 84 (64-121) years, which is consistent with the inverse modeling within the estimated error.

Regarding CCl_4, the best estimate of the stratospheric lifetime is 42 (33-58) years, again based on a stratospheric lifetime of 53.8 years for CFC-11. This is slightly larger than the previous estimate of 35 years discussed in Montzka and Reimann (2011). Based on updated estimates of the other loss processes (oceanic uptake and degradation in soils) a new best estimate of the CCl_4 lifetime is 24 (18-40) years, which is slightly smaller than the value of 26 years suggested in Montzka and Reimann (2011). The discrepancy in emissions estimated using bottom-up and top-down-techniques (see discussion in Montzka and Reimann (2011)) cannot be resolved using this new estimate.

The main loss process for HCFC is reaction with OH radicals in the troposphere. Based on the tropospheric OH levels estimated from the inversion of CH_3CCl_3, on new recommendations for the OH reaction rate coefficients and on stratospheric lifetimes (see Chapter 3), the steady-state global lifetimes (see Tables 4.3 and 4.9) and the tropospheric lifetimes (Table 4.3) have been calculated for a range of HCFCs and HFCs. The resulting global lifetimes are 12.4, 9.4, and 17.7 years for HCFC 22, 141b, and 142b, respectively. One new study (Laube *et al.,* 2013) suggests that the stratospheric lifetime of HCFC-22 should be 3.06 (1.31-∞) times larger than that of CFC-11, i.e., 165 years (70-∞). The other HCFCs for which new result on the stratospheric lifetime are available are HCFC-141b and HCFC-142b, which should have stratospheric lifetime 2.02 (0.82-∞) and 6.75 (1.39-∞) times longer than that of CFC-11, respectively. Using the reference stratospheric lifetime of 53.8 years for CFC-11 results in stratospheric lifetimes of 109 (44-∞) and 363 (75-∞) years for HCFC-141b and HCFC-142b, respectively.

For Halon-1211, our best estimate for the stratospheric lifetime is 31 (24-45) years. Laube *et al.* (2013) further suggest that Halon-1301 should have a stratospheric lifetime that is 1.37 (1.13-1.74) times longer than that of CFC-11, i.e., 74 (56-106) years. Newland *et al.* (2012)

report model estimates of the stratospheric lifetimes for Halon-2402 and Halon-1202 of 31 (27-37) and 21 (18-26) years, respectively, which are consistent with stratospheric observations.

The best estimate for the stratospheric lifetime of CH_3CCl_3 is 0.74 (0.57-1.04) times that of CFC-11, resulting in a stratospheric lifetime of 40 (29-63) years. The inverse modeling by Rigby *et al.* (2013) suggests that the global lifetime of CH_3CCl_3 is 5.04 (4.75-5.37) years (average of inversion using NOAA and AGAGE data), in good agreement with the current WMO recommendation of 5.0 years.

While there have been some variations in the predicted lifetimes of CH_3Cl and CH_3Br, the overall ranges are 0.7-1.3 years for CH_3Cl and 0.6-1.1 years for CH_3Br, with best estimates being 0.9 and 0.8 (0.7-0.9) years respectively. New information is providing only small adjustments to the estimated lifetime. The current best estimates are unchanged from WMO (2011): 1 year for CH_3Cl and 0.8 year for CH_3Br.

Table 4.10 includes estimated lifetimes for N_2O, based on the observational lifetime methods discussed above. A value of 146 (111-212) years for the stratospheric lifetime is derived from the best estimate of the lifetime ratio studies. The IPCC 2007 recommendation of 114 years is near the low end of this range. A lifetime of 116 (85-181) years, based on CLAES N_2O observations with updated photochemical calculations (Minschwaner *et al.,* 1998, 2013), suggests about this lifetime and is consistent within the 2σ range of the correlation studies. The global steady-state lifetime of methane (CH_4) has been calculated to be 9.8 (7.6-13.8) years based on the tropospheric OH levels from the inversion of CH_3CCl_3 and recommendations for the OH reaction rate coefficients and stratospheric lifetimes from Chapter 3 of this report.

Reliable estimates of the atmospheric lifetimes of trace gases require high-quality observations as stated above. It should be ensured that these networks and continued stratospheric observations are maintained in order to provide the necessary reliable data for existing trace gases and also for new species as they appear. In addition air archives like the one from the Cape Grim observatory provide an invaluable database for future studies. Next to the knowledge of the temporal development of a species, good knowledge of the atmospheric loss and the sources to the atmosphere (both natural and anthropogenic emissions) are key in improving our knowledge on the atmospheric lifetimes of radiatively important or ozone depleting trace gases in the atmosphere. For this aspect, better estimates of emissions and better knowledge of the atmospheric chemistry and photochemistry are needed. Also, applying the methods used to derive information on atmospheric lifetimes from observation to model data may help in evaluating the methods used.

Table 4.9. Summary of estimated global lifetimes (years) (mean and 2-σ standard deviation) from various approaches described in this chapter, and previously recommended by WMO and IPCC. All values are steady-state lifetimes or have been adjusted for tracer transience, with the exception of the global box modeling results, which are, however, expected to be good proxies of the steady-state lifetimes.

	WMO 2011, IPCC 2007*	**WMO 1994**	**Inverse AGAGE and NOAA**[b]	**Global Box Model**	**Satellite derived**[c]	**Tracer Correlations**[d] **(best estimate)**
N_2O	114[*]				116 (85-181)	146 (111-212)
CH_4	12[*a]		9.8 (7.6-13.8)			
CFC-11	45	50	53 (40-72)		45 (30-91)	N.A.
CFC-12	100	102	111 (79-157)		107 (79-166)	103 (81-140)
CFC-113	85	85	109 (87-137)			84 (64-121)
CH_3CCl_3	5	5.4	5.04 (4.75-5.37)			
HCFC-22	11.9		12.4 (9.3-18.5)			
CH_3Br	0.8	1.3		0.8 (0.7-0.9)		
CH_3Cl	1	1.5		0.9		
CCl_4	26	42		24 (18-40)		
Halon-1301	65	65				74 (56-106)
HCFC-141b			9.4 (7.2-13.6)			
HCFC-142b			17.7 (12.7-29.2)			
HFC-23	222		228 (160-393)			
HFC-32	5.2		5.4 (4-8.1)			
HFC-125	28.2		30.5 (22.2-48.9)			
HFC-134a	13.4		13.5 (9.9-21.2)			
HFC-143a	47.1		51.4 (37.7-80.4)			
HFC-152a	1.5		1.6 (1.2-2.2)			
HFC-227ea	38.9		35.8 (25.4-60.7)			
HFC-245fa	7.7		7.9 (5.5-13.8)			

[a] In the case of CH_4 the given value is a response time, which is different from the steady-state lifetime.

[b] Only values for CFC-11, CFC-12, CFC-113 and CH_3CCl_3 are from inversion. The lifetimes given for other species in this column are from a forward run of the model using the OH fields derived from the CH_3CCl_3 inversion and stratospheric loss rates based on modeling work in Chapter 5.

[c] The satellite-derived values are the same as given in Table 4.10 for N_2O, CFC-12, and CFC-113, as these have no significant tropospheric loss.

[d] The values in this column are for the species from Table 4.10, for which the stratospheric lifetime is assumed to be equal to the global lifetime, i.e., tropospheric loss is negligible. All values based on an assumed stratospheric CFC-11 lifetime of 53.8 years.

Table 4.10. Best estimates of stratospheric lifetimes of trace-gases. The best estimate from the correlation studies is based on an assumed stratospheric CFC-11 lifetime of 53.8 (44.3-68.8) years and the average ratios shown in Table 4.8. Only data for CFCs are shown from the inversion studies, as the global and the stratospheric lifetimes are assumed to be equal for these species. All uncertainties are 2-σ errors. All values are representative of steady-state lifetimes.

	WMO 2011	**WMO 1994**	**Inverse AGAGE and NOAA**	**Satellite derived**	**Tracer Correlations (best estimate)**	**2D Model checked for consistency with observations**
N_2O	114*	120		116 (85-181)	146 (111-212)	
CH_4						
CFC-11	45	50			N.A.	
CFC-12	100	102	111 (79-157)	107 (79-166)	103 (81-140)	
CFC-113	85	85	109 (87-137)		84 (64-121)	
CH_3CCl_3	39				40 (29-63)	
HCFC-22	186				165 (70-∞)	
CH_3Br						
CH_3Cl					83 (28-∞)	
CCl_4	35				42 (33-58)	
Halon-1211					31 (24-45)	
Halon-1301	65	65			74 (56-106)	
Halon-2402						31 (27-37)
Halon-1202						21 (18-26)
HCFC-141b	64.9				109 (44-∞)	
HCFC-142b	160				363 (75-∞)	

4.6 References

Allen, N. D. C., P. F. Bernath, C. D. Boone, M. P. Chipperfield, D. Fu, G. L. Manney, D. E. Oram, G. C. Toon, and D. K. Weisenstein, Global carbon tetrachloride distributions obtained from the Atmospheric Chemistry Experiment (ACE), Atmos. Chem. Phys., 9, 7449-7459, 2009.

Andrews, A. E., K. A. Boering, S. C. Wofsy, B. C. Daube, D. B. Jones, S. Alex, M. Loewenstein, J. R. Podolske, and S. E. Strahan, Empirical age spectra for the midlatitude lower stratosphere from *in situ* observations of CO_2, *J. Geophys. Res.*, *106,* 10257-10274, 2001.

Avallone, L. M., and M. J. Prather, Tracer-tracer correlations: three-dimensional model simulations and comparisons to observations, *J. Geophys. Res.*, *102*, 19233-19246, 1997.

Atkinson, R., D. L. Baulch, R. A. Cox, J. N. Crowley, R. F. Hampson, R. G. Hynes, M. E. Jenkin, M. J. Rossi, J. Troe, and IUPAC Subcommittee, Evaluated kinetic and photochemical data for atmospheric chemistry: Volume II – gas phase reactions of organic species, *Atmos. Chem. Phys*., 6, 3625-4055, doi: 10.5194/acp-6-3625-2006, 2006.

Atkinson, R., D. L. Baulch, R. A. Cox, J. N. Crowley, R. F. Hampson, R. G. Hynes, M. E. Jenkin, M. J. Rossi, J. Troe, and T. J. Wallington, Evaluated kinetic and photochemical data for atmospheric chemistry, *Atmos. Chem. Phys*., 8, 4141-4496, 2008.

Bernath, P. F., Atmospheric Chemistry Experiment (ACE): Analytical chemistry from orbit, *Trends in Analytical Chemistry 2006, 25*, 647-54, 2006.

Bernath, P. F., C. T. McElroy, M. C. Abrams, C. D. Boone, M. Butler, C. Camy-Peyret, M. Carleer, C. Clerbaux, P.-F. Coheur, R. Colin, P. DeCola, M. DeMazière, J. R. Drummond, D. Dufour, W. F. J. Evans, H. Fast, D. Fussen, K. Gilbert, D. E. Jennings, E. J. Llewellyn, R. P. Lowe, E. Mahieu, J. C. McConnell, M. McHugh, S. D. McLeod, R. Michaud, C. Midwinter, R. Nassar, F. Nichitiu, C. Nowlan, C. P. Rinsland, Y. J. Rochon, N. Rowlands, K. Semeniuk, P. Simon, R. Skelton, J. J. Sloan, M.-A. Soucy, K. Strong, P. Tremblay, D. Turnbull, K. A. Walker, I. Walkty, D. A. Wardle, V. Wehrle, R. Zander, and J. Zou., Atmospheric Chemistry Experiment ACE): Mission overview, *Geophys. Res. Lett, 32*, L15S01, doi: 10.1029/2005GL022386, 2005.

Bingham, G. E., D. K. Zhou, B. Y. Bartschi, G. P. Anderson, D. R. Smith, J. H. Chetwynd, and R. M. Nadile, Cryogenic Infrared Radiance Instrumentation for Shuttle (CIRRIS-1A) Earth limb spectral measurements, calibration, and atmospheric O_3, HNO_3, CFC-12, and CFC-11 profile retrieval, *J. Geophys. Res.*, *102*, 3547-3558, 1997.

Blei, E., C. J. Hardacre, G. P. Mills, K. V. Heal, and M. R. Heal, Identification and quantification of methyl halide sources in a lowland tropical rainforest, *Atmos. Environ.*, *44*(8), 1005-1010, 2010.

Brown, A. T., C. M. Volk, M. R. Schoeberl, C. D. Boone, and P. F. Bernath, Stratospheric lifetimes of CFC-12, CCl_4, CH_4, CH_3Cl, and N_2O from measurements made by the Atmospheric Chemistry Experiment-Fourier Transform Spectrometer (ACE-FTS), *Atmos. Chem. Phys. Discuss*., 13, 4221–4287, doi:10.5194/acpd-13-4221-2013, 2013.

Brown, A. T., M. P. Chipperfield, C. Boone, C. Wilson, K. A. Walker, and P. F. Bernath, Trends in atmospheric halogen containing gases since 2004, *J. Quant. Spectrosc. Radiat. Trans*., *112,* 2552-2566, 2011.

Buizert, C., P. Martinerie, V. V. Petrenko, J. P. Severinghaus., C. M. Trudinger, E. Witrant, J. L. Rosen, A. J. Orsi, M. Rubino, D. M. Etheridge, L. P. Steele, C. Hogan, J. C. Laube, W. T. Sturges, V. A. Levchenko, Smith, A. M., Levin, I., Conway, T. J. Dlugokencky, E. J., Lang, P. M., Kawamura, K., T. M. Jenk, J. W. C. White, T. Sowers, J. Schwander, and T. Blunier, Gas transport in firn: Multiple-tracer characterisation and model intercomparison for NEEM, Northern Greenland, *Atmos. Chem. Phys*., *12*, 4259-4277, doi: 10.5194/acp-12-4259-2012, 2012.

Bujok, O., V. Tan, E. Klein, R. Nopper, R. Bauer, A. Engel, M.-T. Gerhards, A. Afchine, D. S. McKenna, U. Schmidt, F. G. Wienhold, and H. Fischer, GHOST—A novel airborne gas chromatograph for *in situ* measurements of long-lived tracers in the lower stratosphere: Method and applications*, J. Atmos. Chem., 39*, 37-64, 2001.

Butler, J. H., The potential role of the ocean in regulating atmospheric CH_3Br. *Geophys. Res. Lett., 21*, 185-188, 1994.

Butler, J. H., J. W. Elkins, T. M. Thompson, and B. D. Hall, Oceanic consumption of CH_3CC1_3: Implications for tropospheric OH*, J. Geophys. Res., 96D*, 22347-22355, 1991.

Butler, J. H., S. A. Yvon-Lewis, J. M. Lobert, D. B. King, S. A. Montzka, J. W. Elkins, B. D. Hall, and V. Koropalov, A revised look at the oceanic sink for atmospheric CCl_4, *E.O.S. Trans. Fall Suppl*., A51A-0273, 2011.

Chang, A. Y., R. J. Salawitch, H. A. Michelsen, M. R. Gunson, M. C. Abrams, R. Zander, C. P. Rinsland, J. W. Elkins, G. S. Dutton, C. M. Volk, C. R. Webster, R. D. May, D. W. Fahey, R.-S. Gao, M. Loewenstein, J. R. Podolske, R. M. Stimpfle, D. W. Kohn, M. H. Proffitt, J. J. Margitan, K. R. Chan, M. M. Abbas, A. Goldman, F. W. Irion, G. L. Manney, M. J. Newchurch, and G. P. Stiller, A comparison of measurements from ATMOS and Instruments aboard the ER-2 aircraft: Halogenated gases, *Geophys. Res. Lett.*, *23*, 2393-2396, 1996.

Crutzen, P. J., and U. Schmailzl, Chemical budgets of the stratosphere, *Planet. Space Sci*., *31*, 1009-1032, 1983.

Cunnold, D. M., P. J. Fraser, R. F. Weiss, R. G, Prinn, P. G. Simmonds, B. R. Miller, F. N. Alyea, *et al.,* Global trends and annual releases of CCI_3F and CCI_2F_2 estimated from ALE/GAGE and other measurements from July 1978 to June 1991, *J. Geophys. Res*., *99* (D1), 1107-1126, 1994.

Cunnold, D. M., R. G. Prinn, R. A. Rasmussen, P. G. Simmonds, F. N. Alyea, C. A. Cardelino, A. J. Crawford, P. J. Fraser, and R. D. Rosen, The Atmospheric Lifetime Experiment. 3. Lifetime methodology and application to three years of $CFCI_3$ data, *J. Geophys. Res., 88*, 8379-8400, 1983.

Cunnold, D. M., R. F. Weiss, R. G. Prinn, D. E. Hartley, P. G. Simmonds, P. J. Fraser, B. R. Miller, F. N. Alyea, and L. Porter, GAGE/AGAGE measurements indicating reductions in global emissions of CCl_3F and CCl_2F_2 in 1992-1994, *J. Geophys. Res., 102*, 1259-1269, 1997.

Dimmer, C. H., P. G. Simmonds, G. Nickless, and M. R. Bassford, Biogenic fluxes of halomethanes from Irish peatland ecosystems, *Atmos. Environ.*, *35* (2), 321-330, 2001.

Douglass, A. R., R. S. Stolarski, M. R. Schoeberl, C. H. Jackman, M. L. Gupta, P. A. Newman, J. E. Nielsen, and E. L. Fleming, Relationship of loss, mean age of air and the distribution of CFCs to stratospheric circulation and implications for atmospheric lifetimes*, J. Geophys. Res., 113*, D14309, doi: 10.1029/2007JD009575, 2008.

Dufour, G., C., D. Boone, and P. F. Bernath, First measurements of CFC-113 and HCFC-142b from space using ACE-FTS infrared spectra. *Geophys. Res. Lett.*, *32*, 4, 2005.

Ehhalt, D. H., F. Rohrer, D. R. Blake, D. E. Kinnison, and P. Konopka, On the use of nonmethane hydrocarbons for the determination of age spectra in the lower stratosphere, *J. Geophys. Res.*, *112*, D12208, doi: 10.1029/2006JD007686, 2007.

Flocke, F., R. L. Herman, R. J. Salawitch, E. Atlas, C. R. Webster, S. M. Schauffler, R. A. Lueb, R. D. May, E. J. Moyer, K. H. Rosenlof, D. C. Scott, D. R. Blake, and T. P. Bui, An examination of chemistry and transport processes in the tropical lower stratosphere using observations of long-lived and short-lived compounds obtained during STRAT and POLARIS, *J. Geophys. Res.*, *104*, 26625-26642, doi: 10.1029/1999JD900504, 1999.

Greenblatt, J. B., H.-J. Jost, M. Loewenstein, J. R. Podolske, D. F. Hurst, J. W. Elkins, S. M. Schauffler, E. L. Atlas, R. L. Herman, C. R. Webster, T. P. Bui, F. L. Moore, E. A. Ray, S. Oltmans, H. Vömel, J.-F. Blavier, B. Sen, R. A. Stachnik, G. C. Toon, A. Engel, M. Müller, U. Schmidt, H. Bremer, R. B. Pierce, B.-K. Sinnhuber, M. Chipperfield, and F. Lefevre, Tracer-based determination of vortex descent in the 1999/2000 Arctic winter, *J. Geophys. Res., 107*, doi: 10.1029/2001JD000937, 2002.

Grooß, J.-U., and J. M. Russell III, Technical note: A stratospheric climatology for O_3, H_2O, CH_4, NO_x, HCl, and HF derived from HALOE measurements, *Atmos. Chem. Phys.*, *5*, 2792-2807, 2005.

Grossmann, K. U., D. Offermann, O. Gusev, J. Oberheide, M. Riese, and R. Spang, The CRISTA-2 mission, *J. Geophys. Res.*, *107*, 8173, 2002.

Hall, T. M., and R. A. Plumb, Age as a diagnostic of stratospheric transport. *J. Geophys. Res.*, *99*, 1059-1069, 1994.

Happell, J. D., and M. P. Roche, Soils: A global sink of atmospheric carbon tetrachloride, *Geophys. Res. Lett., 30 (2),* 1088, doi: 10:1029/2002GL015957, 2003.

Herman, R. L., K. Drdla, J. R. Spackman, D. F. Hurst, P. J. Popp, C. R. Webster, P. A. Romashkin, J. W. Elkins, E. M. Weinstock, B. W. Gandrud, G. C. Toon, M. R. Schoeberl, H. Jost, E. L. Atlas, and T. P. Bui, Hydration, dehydration, and the total hydrogen budget of the 1999/2000 winter Arctic stratosphere, *J. Geophys. Res.*, *107*, doi: 10.1029/2001JD001257, 2003.

Herman, R. L., D. C. Scott, C. R. Webster, R. D. May, E. J. Moyer, R. J. Salawitch, Y. L. Yung, G. C. Toon, B. Sen, J. J. Margitan, K. H. Rosenlof, H. A. Michelsen, and J. W. Elkins, Tropical entrainment time scales inferred from stratospheric N_2O and CH_4 observations, *Geophys. Res. Lett.*, *25*, 2781-2784, 1998.

Hoffmann, L., R. Spang, M. Kaufmann, and M. Riese, Retrieval of CFC-11 and CFC-12 from Envisat MIPAS observations by means of rapid radiative transfer calculations, *Adv. Space Res., 36*, 915-921, 2005.

Hoffmann, L., M. Kaufmann, R. Spang, R. Müller, J. J. Remedios, C. M. Volk, T. von Clarmann, and M. Riese, Envisat MIPAS measurements of CFC-11: Retrieval, validation, and climatology, *Atmos. Chem. Phys.*, *8*, 3671-3688, 2008.

Homan, C. D., Volk, C. M., Kuhn, A. C., Werner, A., Baehr, J., Viciani, S., Ulanovski, A., and Ravegnani, F., Tracer measurements in the tropical tropopause layer during the AMMA/SCOUT-O3 aircraft campaign, *Atmos. Chem. Phys*., 10, 3615-3627, doi: 10.5194/acp-10-3615-2010, 2010.

Hu, L., S. A. Yvon-Lewis, Y. Liu, J. Salisbury, and J. E. O'Hern, Coastal emissions of methyl bromide and methyl chloride along the eastern Gulf of Mexico and east coast of the U.S., *Global Biogeochem. Cycles*, *24*, GB1007, doi: 10.1029/2009GB003514, 2010.

Hu, L., S. A. Yvon-Lewis, Y. Liu, and T. S. Bianchi, The ocean in near equilibrium with atmospheric CH_3Br, *Global Biogeochem. Cycles*, GB3016, doi: 10.1029/2011GB004272, 2012.

Hu, L., S. A. Yvon-Lewis, J. H. Butler, D. B. King, J. Lobert, and S. A. Montzka, An improved oceanic budget for methyl chloride, *J. Geophys. Res.*, 118, doi: 10.1029/2012JC008196, 2013.

IPCC (Intergovernmental Panel on Climate Change), *Climate Change 2007: The Physical Science Basis*, *Contribution of Working Group I to the Fourth Assessment Report of the Intergovernmental Panel on Climate Change*, edited by S. Solomon, D. Qin, M. Manning, Z. Chen, M. Marquis, K. B. Averyt, M. Tignor, and H. L. Miller, 996 pp., Cambridge University Press, Cambridge, U.K., and New York, NY, U.S.A., 2007.

Irion, F. W., M. R. Gunson, G. C. Toon, A. Y. Chang, A. Eldering, E. Mahieu, G. L. Manney, H. A., Michelsen, E. J. Moyer, M. J. Newchurch, G. B. Osterman, C. P. Rinsland, R. J. Salawitch, B. Sen, Y. L. Yung, and R. Zander, Atmospheric Trace Molecule Spectroscopy (ATMOS) Experiment Version 3 data retrievals, *Appl. Opt., 41*, 6968-6979, 2002.

Jobson, B. T., S. A. McKeen, D. D. Parrish, F. C. Fehsenfeld, D. R. Blake, A. Goldstein, S. Schauffler, and J. Elkins, Trace gas mixing ratio variability vs. lifetime in the troposphere and Stratosphere - Observations, *J. Geophys. Res., 104*, 16091-16113, 1999.

Johnston, H. S., O. Serang, and J. Podolske, Instantaneous global nitrous oxide photochemical rates, *J. Geophys. Res.*, *84,* 5077-5082, 1979.

Jost, H.-J., M. Loewenstein, J. B. Greenblatt, J. R. Podolske, T. P. Bui, D. F. Hurst, J. W. Elkins, R. L. Herman, C. R. Webster, S. M. Schauffler, E. L. Atlas, P. A. Newman, L. R. Lait, and S. C. Wofsy, Mixing events revealed by anomalous tracer relationships in the Arctic vortex during winter 1999/2000, *J. Geophys. Res.*, *107*, doi: 10.1029/2002JD002380, 2002.

Kaye, J., S. A. Penkett, and F. M. Ormond, *Report on Concentrations, Lifetimes, and Trends of CFCs, Halons, and Related Specie*s, NASA Reference Publication 1339, January, 247 pp., 1994.

Keene, W. C., M. A. K. Khalil, D. J. Erickson, III, A. McCulloch, T. E. Graedel, J. M. Lobert, M. L. Aucott, S. L. Gong, D. B. Harper, G. Kleiman, P. Midgley, R. M. Moore, C. Seuzaret, W. T. Sturges, C. M. Benkovitz, V. Koropalov, L. A. Barrie, and Y. F. Li, Composite global emissions of reactive chlorine from anthropogenic and natural sources: Reactive Chlorine Emissions Inventory, *J. Geophys. Res.*, *104* (D7), 8429-8440, 1999.

Keppler, F., D. B. Harper, T. Röckmann, R. M. Moore, and J. T. G. Hamilton, New insight into the atmospheric chloromethane budget gained using stable carbon isotope ratios, *Atmos. Chem. Phys.*, *5* (9), 2403-2411, 2005.

King, D. B., and E. S. Saltzman, Removal of methyl bromide in coastal seawater: Chemical and biological rates, *J. Geophys. Res.*, *102* (C8), 18715-18721, 1997.

Ko, M. K. W., N. D. Sze, and D. K. Weisenstein, Use of satellite data to constrain the model-calculated atmospheric lifetime for N_2O: Implications for other grace gases, *J. Geophys. Res.*, *96*, 7547-7552, 1991.

Krysell, M., E. Fogelqvist, and T. Tanhua, Apparent removal of the transient tracer carbon tetrachloride from anoxic seawater, *Geophys. Res. Lett.*, *21* (23), 2511-2515, 1994.

Kuell, V., D. Offermann, M. Jarisch, B. Schaeler, A. Engel, H. Claude, H. G. J. Smit, A. Ebel, and H. Feldmann, Tropopause region temperatures and CFC 11 mixing ratios from CRISTA 2, *J. Geophys. Res., 110*, D16104, doi: 10.1029/2004JD005592, 2005.

Laube, J. C., A. Engel, H. Bönisch, T. Möbius, D. R. Worton, W. T. Sturges, K. Grunow, and U. Schmidt, Contribution of very short-lived organic substances to stratospheric chlorine and bromine in the tropics – a case study, *Atmos. Chem. Phys.*, *8*, 7325-7334, doi: 10.5194/acp-8-7325-2008, 2008.

Laube, J. C., A. Engel, H. Bönisch, T. Möbius, W. T. Sturges, M. Braß, and T. Röckmann, Fractional release factors of long-lived halogenated organic compounds in the tropical stratosphere, *Atmos. Chem. Phys.*, *10*, 1093-1103, doi: 10.5194/acp-10-1093-2010, 2010a.

Laube, J. C., P. Martinerie, E. Witrant, T. Blunier, J. Schwander, C. A. M. Brenninkmeijer, T. J. Schuck, M. Bolder, T. Röckmann, C. van der Veen, H. Bönisch, A. Engel, G. P. Mills, M. J. Newland, D. E. Oram, C. E. Reeves, and W. T. Sturges, Accelerating growth of HFC-227ea (1,1,1,2,3,3,3-heptafluoropropane) in the atmosphere, *Atmos. Chem. Phys.*, *10*, 5903-5910, doi: 10.5194/acp-10-5903-2010, 2010b.

Laube, J. C., A. Keil., H. Bönisch, A. Engel, T. Röckmann, C.M. Volk, and W. T. Sturges, Observation-based assessment of stratospheric fractional release, lifetimes, and Ozone Depletion Potentials of ten important source gases, *Atmos. Chem. Phys.,* 13, doi: 10.5194/acp-13-2779-2013, 2779-2791, 2013.

Lee, B.-S., J. L. Bullister, and F. A. Whitney, Chlorofluorocarbon CFC-11 and carbon tetrachloride removal in Saanich Inlet, an intermittently anoxic basin, *Marine Chem.*, *66*, 171-185, 1999.

Lee-Taylor, J. M., and E. A. Holland, Litter decomposition as a potential natural source of methyl bromide, *J. Geophys. Res.*, *105* (D7), 8857-8864, 2000.

Lee-Taylor, J., and K. R. Redeker, Reevaluation of global emissions from rice paddies of methyl iodide and other species, *Geophys. Res. Lett.*, *32*, L15801, doi: 0.1029/2005GL022918, 2005.

Liu, X.-F., Evidence of biodegradation of atmospheric carbon tetrachloride in soils: Field and microcosm studies, Ph.D. Thesis, 139pp. Columbia University, New York, NY U.S.A, 2006.

Lobert, J. M., W. C. Keene, J. A. Logan, and R. Yevich, Global chlorine emissions from biomass burning: Reactive Chlorine Emissions Inventory, *J. Geophys. Res.*, *104* (D7), 8373-8389, 1999.

Mahieu, E., P. Duchatelet, P. Demoulin, K. A. Walker, E. Dupuy, and L. Froidevaux, Validation of ACE-FTS v2.2 measurements of HCl, HF, CCl_3F and CCl_2F_2 using space-, balloon- and ground-based instrument observations, *Atmos. Chem. Phys., 8*, 6199-6221, 2008.

Maiss, M., L. P. Steele, R. J. Francey, P. J. Fraser, R. L. Langenfelds, N. B. A. Trivett, and I. Levin, Sulfur hexafluoride – a powerful new atmospheric tracer, *Atmos. Environ.*, *30,* 1621-1629, 1996.

Manley, S. L., N.-Y. Wang, M. L. Walser, and R. J. Cicerone, Methyl halide emissions from greenhouse-grown mangroves, *Geophys. Res. Lett.*, *34* (1), L01806, 2007.

Martinerie, P., E. Nourtier-Mazauric, J.-M. Barnola, W. T. Sturges, D. R. Worton, E. Atlas, L. K. Gohar, K. P. Shine, and G. P. Brasseur, Long-lived halocarbon trends and budgets from atmospheric chemistry modelling constrained with measurements in polar firn, *Atmos. Chem. Phys.*, *9*, 3911-3934, 2009.

McCulloch, A., P. Ashford, and P. M. Midgley, Historic emissions of fluorotrichloromethane (CFC-11) based on a market survey. *Atmos. Environ.*, *35* (26), 4387-4397. doi: 10.1016/S1352-2310(01)00249-7, 2001.

McCulloch, A., P. M. Midgley, and P. Ashford, Releases of refrigerant gases (CFC-12, HCFC-22 and HFC-134a) to the atmosphere. *Atmos. Environ.*, *37* (7), 889-902, doi: 10.1016/S1352-2310(02)00975-5, 2003.

Mead, M. I., I. R. White, G. Nickless, K.-Y. Wang, and D. E. Shallcross, An estimation of the global emission of methyl bromide from rapeseed (Brassica napus) from 1961 to 2003, *Atmos. Environ.*, 42 (2), 337-345, 2008a.

Mead, M. I., M. A. H. Khan, G. Nickless, B. R. Greally, D. Tainton, T. Pitman, and D. E. Shallcross, Leaf cutter ants: A possible missing source of biogenic halocarbons, *Environ. Chem.*, *5* (1), 5-10, 2008b.

Mellouki, A., R. K. Talukdar, A.-M. Schmoltner, T. Gierczak, M. J. Mills, S. Solomon and A. R. Ravishankara, Atmospheric lifetimes and ozone depletion potentials of methyl bromide (CH_3Br) and dibromomethane (CH_2Br_2), *Geophys. Res. Lett., 19* (22), 2279-2280, 1992.

Minschwaner, K., R. J. Salawitch, and M. B. McElroy, Absorption of solar radiation by O_2: Implications for O_3 and lifetimes of N_2O, $CFCl_3$, and CF_2Cl_2, *J. Geophys. Res.*, *98*, 10543-10561, 1993.

Minschwaner, K., R. W. Carver, B. P. Briegleb, and A. E. Roche, Infrared radiative forcing and atmospheric lifetimes of trace species based on observations from UARS, *J. Geophys. Res.*, *103*, 23243-23253, 1998.

Minschwaner, K., L. Hoffmann, A. Brown, M. Riese, R. Müller, and P. B. Bernath, Stratospheric loss and atmospheric lifetimes of CFC-11 and CFC-12 derived from satellite observations, *Atmos. Chem. Phys., 13,* 4253-4263, 2013.

Montzka, S. A., and S. Reimann (Coordinating Lead Authors), A. Engel, K. Krüger, S. O'Doherty, and W. T. Sturges (Lead Authors), Ozone-Depleting Substances (ODSs) and Related Chemicals, Chapter 1 in *Scientific Assessment of Ozone Depletion: 2010,* *Global Ozone Research and Monitoring Project–Report No. 52*, 516 pp., World Meteorological Organization, Geneva, Switzerland, 2011.

Montzka, S. A., M. Krol, E. Dlugokencky, B. Hall, P. Jöckel, and J. Lelieveld, Small interannual variability of global atmospheric hydroxyl, *Science*, *331,* 67-69, 2011.

Moore, D. P., A. M. Waterfall, and J. J. Remedios, The potential for radiometric retrievals of halocarbon concentrations from the MIPAS-E instrument, *Adv. Space Res., 37*, 2238-2246, 2006.

Moore, F. L., J. W. Elkins, E. A. May, G. S. Dutton, R. E. Dunn, D. W. Fahey, R. J. McLaughlin, T. L. Thompson, P. A. Romashkin, D. F. Hurst, and P. R. Wamsley, Balloonborne *in situ* gas chromatograph for measurements in the troposphere and stratosphere, *J. Geophys. Res.*, *108* (D5), 8330, doi: 10.1029/2001JD000891, 2003.

Moore, R. M., W. Groszko, and S. J. Niven, Ocean-atmosphere exchange of methyl chloride: Results from NW Atlantic and Pacific Ocean studies. *J. Geophys. Res., 101,* 28529-28538, 1996.

Mühle, J., A. L. Ganesan, B. R. Miller, P. K. Salameh, C. M. Harth, B. R. Greally, M. Rigby, L. W. Porter, L. P. Steele, C. M. Trudinger, P. B. Krummel, S. O'Doherty, P. J. Fraser, P. G. Simmonds, R. G. Prinn, and R. F. Weiss, Perfluorocarbons in the global atmosphere: tetrafluoromethane, hexafluoroethane, and octafluoropropane, *Atmos. Chem. Phys.,* 10 (11), 5145-5164, *10.5194/*acp-10-5145-2010, 2010.

Naik, V., A. K. Jain, K. O. Patten, and D. J. Wuebbles, Consistent sets of atmospheric lifetimes and radiative forcings on climate for CFC replacements: HCFCs and HFCs, *J. Geophys. Res.*, *105* (D5), 6903-6914, doi: 10.1029/1999JD901128, 2000.

Nassar, R., P. F. Bernath, C. D. Boone, C. Clerbaux, P. F. Coheur, G. Dufour, L. Froidevaux, E. Mahieu, J. C. McConnell, S. D. McLeod, D. P. Murtagh, C. P. Rinsland, K. Semeniuk, R. Skelton, K. A. Walker, and R. Zander, A global inventory of stratospheric chlorine in 2004, *J. Geophys. Res.-Atmos., 111*, 13, doi: 10.1029/2006JD007073, 2006a.

Nassar, R., P. F. Bernath, C. D. Boone, S. D. McLeod, R. Skelton, and K. A. Walker, A global inventory of stratospheric fluorine in 2004 based on Atmospheric Chemistry Experiment Fourier transform spectrometer (ACE-FTS) measurements. *J. Geophys. Res.-Atmos., 111*, 10, 2006b.

Newland, M. J., C. E. Reeves, D. E. Oram, J. C. Laube, W. T. Sturges, C. Hogan, and P. J. Fraser, Southern hemispheric halon trends and global halon emissions, 1978-2011, submitted to *Atmos. Chem. Phys. Discuss.,* Sept., 2012.

Nightingale, R. W., Q. E. Roche, J. B. Kumer, J. L. Mergenthaler, J. C. Gille, S. T. Massie, P. L. Bailey, D. P. Edwards, M. R. Gunson, G. C. Toon, B. Sen, J.-F. Blavier, and P. S. Connell, Global CF_2Cl_2 measurements by UARS cryogenic limb array etalon spectrometer: Validation by correlative data and a model, *J. Geophys. Res.*, *101*, 9711-9736, 1996.

Oram, D. E., C. E. Reeves, S. A. Penkett, and P. J. Fraser, Measurements of HCFC−142b and HCFC−141b in the Cape Grim air Archive: 1978–1993, *Geophys. Res. Lett.*, *22* (20), 2741-2744, doi: 10.1029/95GL02849, 1995.

Oram, D. E., W. T. Sturges, S. A. Penkett, A. McCulloch, and P. J. Fraser, Growth of fluoroform (CHF_3, HFC−23) in the background atmosphere, *Geophys. Res. Lett.*, *25* (1), 35-38, doi: 10.1029/97GL03483, 1998.

Park, J. H., M. K. W. Ko, C. H. Jackman, R. A. Plumb, J. A. Kaye, and K. H. Sage, (Eds.), *Models and Measurements Intercomparison II*, Hampton, VA, National Aeronautics and Space Administration, 1999.

Park, S., E. L. Atlas, R. Jiménez, B. C. Daube, E. W. Gottlieb, J. Nan, D. B. A. Jones, L. Pfister, T. J. Conway, T. P. Bui, R.-S. Gao, and S. C. Wofsy, Vertical transport rates and concentrations of OH and Cl radicals in the Tropical Tropopause Layer from CO_2 and halocarbons, *Atmos. Chem. Phys. 10*, 6669, 2010.

Park, S. Y., E. L. Atlas, and K. A. Boering, Measurements of N_2O isotopologues in the stratosphere: Influence of transport on the apparent enrichment factors and the isotopologue fluxes to the troposphere, *J. Geophys. Res.*, *109*, D01305, doi: 10.1029/2003JD003731, 2004.

Pfeilsticker, K., W. T. Sturges, H. Bösch, C. Camy-Peyret, M. P. Chipperfield, A. Engel, R. Fitzenberger, M. Müller, S. Payan, and B.-M. Sinnhuber, Lower stratospheric organic and inorganic bromine budget for the Arctic winter 1998/99, *Geophys. Res. Lett.*, *27*(20), 3305-3308, doi: 10.1029/2000GL011650, 2000.

Plumb, I. C., P. F. Vohralik, and K. R. Ryan, Normalization of correlations for atmospheric species with chemical loss, *J. Geophys. Res., 104*, 11723-11732, 1999.

Plumb, R. A., A "tropical pipe" model of stratospheric transport, *J. Geophys. Res.*, *101*, 3957-3972, 1996.

Plumb, R. A., and M. K. W. Ko., Interrelationships between mixing ratios of long-lived stratospheric constituents, *J. Geophys. Res.*, *97*, 10145-10156, 1992.

Plumb, R. A., W. Heres, J. L. Neu, N. Mahowald, J. del Corral, G. C. Toon, E. Ray, F. Moore, and A. E. Andrews, Global tracer modeling during SOLVE: High latitude descent and mixing, *J. Geophys. Res., 107*, 8309, doi: 1029/2001JD01023, 2002 (printed 108, D5, 2003).

Prinn, R. G., R. Zander (Lead Authors), D. M. Cunnold, J. W. Elkins, A. Engel, P. J. Fraser, M. R. Gunson, M. K. W. Ko, E. Mahieu, P. M. Midgley, J. M. Russell III, C. M. Yolk, and R. F. Weiss, Long-lived ozone-related compounds, in D. L. Albritton, P. J. Aucamp, G. Mégie, and R. T. Watson, editors, *Scientific Assessment of Ozone Depletion, Global Ozone Research and Monitoring Project, Report No. 44*, Chapter 1, World Meteorological Organization, 1999.

Prinn, R. G., R. F. Weiss, P. J. Fraser, P. G. Simmonds, D. M. Cunnold, F. N. Alyea, S. O'Doherty, P. Salameh, B. R. Miller, J. Huang, R. H. J. Wang, D. E. Hartley, C. Harth, L. P. Steele, G. Sturrock, P. M. Midgley, and A. McCulloch, A history of chemically and radiatively important gases in air deduced from ALE/GAGE/AGAGE, *J. Geophys. Res.*, *115*, 17751-17792, doi: 10.1029/2000JD900141, 2000.

Prinn, R. G., J. Huang, R. F. Weiss, D. M. Cunnold, P. J. Fraser, P. G. Simmonds, A. McCulloch, C. Harth, P. Salameh, S. O'Doherty, R. H. Wang, L. Porter, and B. R. Miller. Evidence for substantial variations of atmospheric hydroxyl radicals in the past two decades, *Science, 292,* 1882-8, ISSN 0036-8075, doi: 10.1126/science.1058673. URL http://www.ncbi.nlm.nih.gov/pubmed/11337586, 2001.

Prinn, R. G., J. Huang, R. F. Weiss, D. M. Cunnold, P. J. Fraser, P. G. Simmonds, A. McCulloch, C. Harth, S. Reimann, P. Salameh, R. H. Wang, L. W. Porter,

B. R. Miller, and P. B. Krummel, Evidence for variability of atmospheric hydroxyl radicals over the past quarter century, *Geophys. Res. Lett., 32,* L07809, doi: 10.1029/2004GL022228, 2005.

Ray, E. A., F. L. Moore, J. W. Elkins, G. S. Dutton, D. W. Fahey, H. Vömel, S. J. Oltmans, and K. H. Rosenlof, Transport into the Northern Hemisphere lowermost stratosphere revealed by *in situ* tracer measurements, *J. Geophys. Res.*, *104* (D21), 26565-26580, 1999.

Ray, E. A., F. L. Moore, J. W. Elkins, D. F. Hurst, P. A. Romashkin, G. S. Dutton, and D. W. Fahey, Descent and mixing in the 1999–2000 northern polar vortex inferred from *in situ* tracer measurements, *J. Geophys. Res.*, *107*, doi: 10.1029/2001JD000961, 2002.

Reeves, C. E., Atmospheric budget implications of the temporal and spatial trends in methyl bromide concentration, *J. Geophys. Res.*, *108*, 4343, doi: 10.1029/2002JD002943, 2003.

Rhew, R. C., Sources and sinks of methyl bromide and methyl chloride in the tallgrass prairie: Applying a stable isotope tracer technique over highly variable gross fluxes, *J. Geophys. Res.*, *116* (G3), G03026, doi: 10.1029/2011jg001704, 2011.

Rhew, R. C., B. R. Miller, and R. F. Weiss, Natural methyl bromide and methyl chloride emissions from coastal salt marshes, *Nature*, *403* (6767), 292-295, 2000.

Rhew, R. C., B. R. Miller, M. K. Vollmer, and R. F. Weiss, Shrubland fluxes of methyl bromide and methyl chloride, *J. Geophys. Res., 106*, 20875-20882, 2001.

Rhew, R. C., B. R. Miller, and R. F. Weiss, Chloroform, carbon tetrachloride and methyl chloroform fluxes in southern California ecosystems, *Atmos. Environ.*, *42* (30), 7135-7140, doi: 10.1016/j.atmosenv.2008.05.038, 2008.

Richard, E. C., K. C. Aikin, A. E. Andrews, B. C. Daube, Jr., C. Gerbig, S. C. Wofsy, P. A. Romashkin, D. F. Hurst, E. A. Ray, F. L. Moore, J. W. Elkins, T. Deshler, and G. C. Toon, Severe chemical ozone loss inside the Arctic polar vortex during winter 1999-2000 inferred from *in situ* airborne measurements, *Geophys. Res. Lett.*, *28*, 2197-2200, doi: 10.1029/2001GL012878, 2001.

Riese, M., R. Sprang, P. Preusse, M. Ern, M. Jarisch, D. Offermann, and K. U. Grossmann, Cryogenic Infrared Spectrometers and Telescopes for the Atmosphere (CRISTA) data processing and atmospheric temperature and trace gas retrieval, *J. Geophys. Res.*, *104*, 16349-16367, 1999.

Rigby, M., R. G. Prinn, S. O'Doherty, S. A. Montzka, A. McCulloch, C. M. Harth, J. Mühle, P. K. Salameh, R. F. Weiss, D. Young, P. G. Simmonds, B. D. Hall, G. S. Dutton, D. Nance, D. J. Mondeel, J. W. Elkins, P. B. Krummel, L. P. Steele, and P. J. Fraser, Re-evaluation of the lifetimes of the major CFCs and CH_3CCl_3 using atmospheric trends,
Atmos. Chem. Phys., 13, 2691-2702, 2013.

Roche, A. E., R. W. Nightingale, J. B. Kumer, J. L. Mergenthaler, C. H. Jackman, and E. L. Fleming, Distribution and seasonal variation of CFCs in the stratosphere: Comparison of satellite global data and a 2-D model, *Adv. Space Res., 21*, 1383-1391, 1998.

Rottman, G. J., T. N. Woods, and W. McClintock, SORCE Solar UV Irradiance Results, *Adv. Space Res.*, *37*, 2, 201-208, doi: 10.1016/j.asr.2005.02.072, 2006.

Sander, S. P., J. Abbatt, J. R. Barker, J. B. Burkholder, R. R. Friedl, D. M. Golden, R. E. Huie, C. E. Kolb, M. J. Kurylo, G. K. Moortgat, V. L. Orkin and P. H. Wine, *Chemical Kinetics and Photochemical Data for Use in Atmospheric Studies, Evaluation No. 17*, JPL Publication 10-6, Jet Propulsion Laboratory, Pasadena, http://jpldataeval.jpl.nasa.gov/, 2011.

Schauffler, S. M., E. L. Atlas, D. R. Blake, F. Flocke, R. A. Lueb, J. M. Lee-Taylor, V. Stroud, and W. Travnicek, Distributions of brominated organic compounds in the troposphere and lower stratosphere, *J. Geophys. Res.*, *104* (D17), 21513-21536, doi: 10.1029/1999JD900197, 1999.

Schauffler, S. M., E. L. Atlas, S. G. Donnelly, A. Andrews, S. A. Montzka, J. W. Elkins, D. F. Hurst, P. A. Romashkin, G. S. Dutton, and V. Stroud, Chlorine budget and partitioning during the Stratospheric Aerosol and Gas Experiment (SAGE) III Ozone Loss and Validation Experiment (SOLVE), *J. Geophys. Res.*, *108* (D5), 4173, doi: 10.1029/2001JD002040, 2003.

Schoeberl, M. R., A. R. Douglass, R. S. Stolarski, S. Pawson, S. E. Strahan, and W. Read, Comparison of lower stratospheric tropical mean vertical velocities, *J. Geophys. Res.*, *113,* D24109, doi: 10.1029/2008JD010221, 2008.

Sen, B., G. B. Osterman, R. J. Salawitch, G. C. Toon, J. J. Margitan, J.-F. Blavier, A. Y. Chang, R. D. May, C. R. Webster, R. M. Stimpfle, G. P. Bonne, P. B. Voss, K. K. Perkins, J. G. Anderson, R. C. Cohen, J. W. Elkins, G. S. Dutton, D. F. Hurst, P. A. Romashkin, E. L. Atlas, S. M. Schauffler, and M. Loewenstein, The budget and partitioning of stratospheric chlorine during the 1997 Arctic summer, *J. Geophys. Res., 104* (D21), 26653-26665, doi: 10.1029/1999JD900245, 1999.

Severinghaus, J. P., M. R. Albert, Z. R. Courville, M. A. Fahnestock, K. Kawamura, S. A. Montzka, J. Mühle, T. A. Scambos, E. Shields, C. A. Shuman, M. Suwa, P. Tans, and R. F. Weiss, Deep air convection in the firn at a zero-accumulation site, central Antarctica*, Earth and Planet. Sci. Lett.*, *293*, 359-367, 2010.

Shorter, J. H., C. E. Kolb, P. M. Crill, R. M. Kerwin, R. W. Talbot, M. E. Hines, and R. C. Harriss, Rapid degradation of atmospheric methyl bromide in soils, *Nature, 377*, 717-719, 1995.

Spackman, J. R., E. M. Weinstock, J. G. Anderson, D. F. Hurst, H.-J. Jost, and S. M. Schauffler, Aircraft observations of rapid meridional transport from the tropical tropopause layer into the lowermost stratosphere: Implications for midlatitude ozone, *J. Geophys. Res.*, *112*, D12308, doi: 10.1029/2006JD007618, 2007.

Spivakovsky, C. M., J. A. Logan, S. A. Montzka, Y. J. Balkanski, M. Foreman-Fowler, D. B. A. Jones, L. W. Horowitz, *et al.,* Three-dimensional climatological distribution of tropospheric OH: Update and evaluation, *J. Geophys. Res.*, *105* (D7), 8931-8980, doi: 10.1029/1999JD901006, 2000.

Sturges, W. T., D. E. Oram, L. J. Carpenter, A. Engel, and S. A. Penkett, Bromoform as a source of bromine to the stratosphere, *Geophys. Res. Lett., 27*, 2081-2084, 2000.

Sturges, W. T., H. P. McIntyre, S. A. Penkett, J. Chappellaz, J. Barnola, R. Mulvaney, E. Atlas, and V. Stroud, Methyl bromide, and other brominated methanes, and methyl iodide in polar firn air, *J. Geophys. Res., 106*, 1595-1606, 2001.

Toon, G. C., J.-F. Blavier, B. Sen, J. J. Margitan, C. R. Webster, R. D. May, D. W. Fahey, R. Gao, L. Del Negro, M. Proffitt, J. Elkins, P. A. Romashkin, D. F. Hurst, S. Oltmans,

E. Atlas, S. Schauffler, F. Flocke, T. P. Bui, R. M. Stimpfle, G. P. Bonne, P. B. Voss, and R. C. Cohen, Comparison of MkIV balloon and ER-2 measurements of atmospheric trace gases, *J. Geophys. Res.*, *104*, 26779-26790, 1999.

Trudinger, C. M., D. M. Etheridge, G. A. Sturrock, P. J. Fraser, P. B. Krummel, and A. McCulloch, Atmospheric histories of halocarbons from analysis of Antarctic firn air: Methyl bromide, methyl chloride, chloroform, and dichloromethane, *J. Geophys. Res.*, *109*, D22310, doi: 10.1029/2004JD004932, 2004.

Varner, R. K., P. M. Crill, and R. W. Talbot, Wetlands: A potentially significant source of atmospheric methyl bromide and methyl chloride, *Geophys. Res. Lett.*, *26* (16), 2433-2435, doi: 10.1029/1999gl900587, 1999.

Velazco, V. A., G. C. Toon, J.-F. L. Blavier, A. Kleinböhl, G. L. Manney, W. H. Daffer, P. F. Bernath, K. A. Walker, and C. Boone, Validation of the Atmospheric Chemistry Experiment by noncoincident MkIV balloon profiles, *J. Geophys. Res., 116,* D06306, doi: 10.1029/2010jd014928, 2011.

Volk, C. M., J. W. Elkins, D. W. Fahey, R. J. Salawitch, G. S. Dutton, J. M. Gilligan, M. H. Proffitt, M. Loewenstein, J. R. Podolske, K. Minschwaner, J. J. Margitan, and K. R. Chan, Quantifying transport between the tropical and midlatitude lower stratosphere, *Science, 272,* 1763-1768, 1996.

Volk, C. M., J. W. Elkins, D. W. Fahey, G. S. Sutton, J. M. Gilligan, M. Loewenstein, J. R. Podolske, K. R. Chan, and M. R. Gunson, Evaluation of source gas lifetimes from stratospheric observations, *J. Geophys. Res.*, *102* (D21), 25543-25564, 1997.

Wamsley, P. R., J. W. Elkins, D. W. Fahey, G. S. Dutton, C. M. Volk, R. C. Myers, S. A. Montzka, J. H. Butler, A. D. Clarke, P. J. Fraser, L. P. Steele, M. P. Lucarelli, E. L. Atlas, S. M. Schauffler, D. R. Blake, F. S. Rowland, W. T. Sturges, J. M. Lee, S. A. Penkett, A. Engel, R. M. Stimpfle, K. R. Chan, D. K. Weisenstein, M. K. W. Ko, and R. J. Salawitch, Distribution of halon-1211 in the upper troposphere and lower stratosphere and the 1994 total bromine budget, *J. Geophys. Res, 103*, 1513-1526, 1998.

Wang, H. J., D. M. Cunnold, L. Froidevaux, and J. M. Russell, A reference model for middle atmosphere ozone in 1992-1993, *J. Geophys. Res.*, *104*, 21629-21643, 1999.

Watling, R., and D. B. Harper, Chloromethane production by wood-rotting fungi and an estimate of the global flux to the atmosphere, *Mycol. Res.*, *102* (7), 769-787, 1998.

Werner, A., C. M. Volk, E. V. Ivanova, T. Wetter, C. Schiller, H. Schlager, and P. Konopka, Quantifying transport into the Arctic lowermost stratosphere, *Atmos. Chem. Phys.*, *10*, 11623-11639, www.atmos-chem-phys.net/10/11623/2010/, doi: 10.5194/acp-10-11623-2010, 2010.

WMO, *Scientific Assessment of Ozone Depletion: 1998, Global Ozone Research and Monitoring Project–Report No. 44*, Geneva, Switzerland, 1999.

WMO, *Scientific Assessment of Ozone Depletion: 2002, Global Ozone Research and Monitoring Project–Report No. 47*, 498 pp., Geneva, Switzerland, 2003.

WMO, *Scientific Assessment of Ozone Depletion: 2006, Global Ozone Research and Monitoring Project - Report No. 50*, Geneva, Switzerland, 2007.

WMO, *Scientific Assessment of Ozone Depletion: 2010, Global Ozone Research and Monitoring Project - Report No. 52*, 516 pp., Geneva, Switzerland, 2011.

Xiao, X., R. G. Prinn, P. J. Fraser, R. F. Weiss, P. G. Simmonds, S. O'Doherty, B. R. Miller, P. K. Salameh, C. M. Harth, P. B. Krummel, A. Golombek, L. W. Porter, J. H. Butler, J. W. Elkins, G. S. Dutton, B. D. Hall, L. P. Steele, R. H. J. Wang, and D. M. Cunnold, Atmospheric three-dimensional inverse modeling of regional industrial emissions and global oceanic uptake of carbon tetrachloride, *Atmos. Chem. Phys.*, *10* (21), 10421-10434, doi: 10.5194/acp-10-10421-2010, 2010a.

Xiao, X., R. G. Prinn, P. J. Fraser, P. G. Simmonds, R. F. Weiss, S. O'Doherty, B. R. Miller, P. K. Salameh, C. M. Harth, P. B. Krummel, L. W. Porter, J. Mühle, B. R. Greally, D. Cunnold, R. Wang, S. A. Montzka, J. W. Elkins, G. S. Dutton, T. M. Thompson, J. H. Butler, B. D. Hall, S. Reimann, M. K. Vollmer, F. Stordal, C. Lunder, M. Maione, J. Arduini, and Y. Yokouchi, Optimal estimation of the surface fluxes of methyl chloride using a 3-D global chemical transport model, *Atmos. Chem. Phys.*, *10*, 5515-5533, doi: 10.5194/acp-10-5515-2010, 2010b.

Yokouchi, Y., T. Machida, L. A. Barrie, D. Toom-Sauntry, Y. Nojiri, Y. Fujinuma, Y. Inuzuka, H. Li, H. Akimoto, and S. Aoki, Latitudinal distribution of atmospheric methyl bromide: Measurements and modeling, *Geophys. Res. Lett., 27* (5), doi: 10.1029/1999GL010884, 2000.

Yvon, S. A., and J. H. Butler, An improved estimate of the oceanic lifetime of atmospheric CH3Br, *Geophys. Res. Lett., 23,* (1), 53-56, 1996.

Yvon-Lewis, S. A., and J. H. Butler, The potential effect of oceanic biological degradation on the lifetime of atmospheric CH_3Br, *Geophys. Res. Lett.*, *24* (10), 1227-1230, 1997.

Yvon-Lewis, S. A., and J. H. Butler, Effect of oceanic uptake on atmospheric lifetimes of selected trace gases, *J. Geophys. Res.-Atmos.*, *107* (D20), 2002.

Yvon-Lewis, S. A., E. S. Saltzman, and S. A. Montzka, Recent trends in atmospheric methyl bromide: Analysis of post-Montreal Protocol variability, *Atmos. Chem. Phys.*, *9* (16), 5963-5974, 2009.

Zander, R., C. P. Rinsland, C. B. Farmer, and R. H. Norton, Infrared spectroscopic measurements of halogenated source gases in the stratosphere with the ATMOS instrument, *J. Geophys. Res.*, *92*, 9836-9850, 1987.